Variability in Coastal Flooding predictions due to forecast errors during Hurricane Arthur

R. Cyriac [a,*], J.C. Dietrich [a], J.G. Fleming [b], B.O. Blanton [c], C. Kaiser [d], C.N. Dawson [e], R.A. Luettich [f]

[a] Dept. of Civil, Construction, and Environmental Engineering, NC State University, Campus Box 7908, 2501 Stinson Drive, 428 Mann Hall, Raleigh, NC, 27695, USA
[b] Seahorse Coastal Consulting, 3103 Mandy Lane, Morehead City, NC, 28557, USA
[c] Renaissance Computing Institute, 100 Europa Drive, Suite 540, Chapel Hill, NC, 27517, USA
[d] School of the Coast and Environment, and Center for Computation & Technology, Louisiana State University, 1079 Digital Media Center, Baton Rouge, LA, 70803, USA
[e] Institute of Computational Engineering and Sciences, The University of Texas at Austin, Austin, TX, 78712, USA
[f] Institute of Marine Sciences, University of North Carolina, 150 Coker Hall, 3431 Arendell St, Morehead City, NC, 28557, USA

ARTICLE INFO

Keywords:
Hurricane Arthur (2014)
ADCIRC
North Carolina
Coastal flooding
Forecast uncertainty
HWind
GAHM

ABSTRACT

Storm surge prediction models rely on an accurate representation of the wind conditions. In this paper, we examine the sensitivity of surge predictions to forecast uncertainties in the track and strength of a storm (storm strength is quantified by the power dissipation of the associated wind field). This analysis is performed using Hurricane Arthur (2014), a Category 2 hurricane, which made landfall along the North Carolina (NC) coast in early July 2014. Hindcast simulations of a coupled hydrodynamic-wave model are performed on a large unstructured mesh to analyze the surge impact of Arthur along the NC coastline. The effects of Arthur are best represented by a post-storm data assimilated wind product with parametric vortex winds providing a close approximation. Surge predictions driven by forecast advisories issued by the National Hurricane Center (NHC) during Arthur are analyzed. The storm track predictions from the NHC improve over time. However, successive advisories predict an unrealistic increase in the storm's strength. Due to these forecast errors, the global root mean square errors of the predicted wind speeds and water levels increase as the storm approaches landfall. The relative impacts of the track and strength errors on the surge predictions are assessed by replacing forecast storm parameters with the best known post-storm information about Arthur. In a "constant track" analysis, Arthur's post storm determined track is used in place of the track predictions of the different advisories but each advisory retains its size and intensity predictions. In a "constant storm strength" analysis, forecast wind and pressure parameters are replaced by corresponding parameters extracted from the post storm analysis while each advisory retains its forecast storm track. We observe a strong correlation between the forecast errors and the wind speed predictions. However, the correlation between these errors and the forecast water levels is weak signifying a non-linear response of the shallow coastal waters to meteorological forcing.

1. Introduction

The coastal communities of North Carolina (NC) are under the constant risk of hurricanes. The State Climate Office of NC estimates that a tropical cyclone makes landfall in NC every 2.5 years (State Climate Office of North Carolina, 2017), and the network of bays, estuaries, sounds and barrier islands that define the NC coastline further increases the vulnerability of its coastal regions to the impacts of storm surge and flooding. Surge levels have ranged from 2 m during recent hurricanes like Isabel (2003) and Irene (2011), to 3 m during Floyd (1999) and to more than 6 m during Hazel (1954). The strong winds, storm surge and rainfall associated with these hurricanes, each differing in track and intensity, have caused damages worth billions of dollars (Barnes, 2013).

Technological advancements in flood forecasting have enabled emergency managers to be better informed about the behavior of a threatening storm and its potential impact on their coastal communities. To provide accurate predictions, flood forecasting systems rely on estimations of the storm parameters (e.g., track, size and intensity), accurate representation of coastal geometry, accurate simulations of meteorological and coastal ocean conditions by numerical models, and

* Corresponding author.
E-mail address: rcyriac@ncsu.edu (R. Cyriac).

https://doi.org/10.1016/j.coastaleng.2018.02.008
Received 25 August 2017; Received in revised form 22 February 2018; Accepted 25 February 2018
Available online 31 March 2018

communication of forecast guidance to policymakers and emergency managers in the coastal counties. Emergency managers use these predictions to prepare coastal communities by issuing appropriate warnings, planning evacuation strategies, managing emergency shelters and estimating potential damage to infrastructure during the hurricane (Cheung et al., 2003).

The ADvanced CIRCulation (ADCIRC) model is an unstructured-mesh, finite-element, hydrodynamic model used to simulate storm surge, tides and riverine flow that has been applied extensively for retrospective and risk based storm surge predictions and validation (Westerink et al., 2008; Bunya et al., 2010; Dietrich et al., 2008, 2010; Blanton et al., 2012a; Lin et al., 2012; Atkinson et al., 2013; Bhaskaran et al., 2013; Murty et al., 2014; Lin and Emmanuel, 2016). ADCIRC comprises the core of the ADCIRC Surge Guidance System (ASGS) that has been deployed to forecast storm surge along the US East and Gulf of Mexico coasts (Fleming et al., 2007; Dresback et al., 2011; Dietrich et al., 2013a). For storm surge simulations, ADCIRC is implemented typically to have basin scale coverage with finest resolution of about 20 m in specific areas of interest. The resulting mesh may have millions of finite elements and thus require substantial computing resources to solve. For example, during Hurricane Arthur (2014), a 5 – day ASGS forecast on 480 processor cores took 34 minutes on an unstructured mesh with 295328 vertices. Individual ADCIRC simulations have higher fidelity than limited-domain, low-resolution simulations (Kerrr et al., 2013), because of the larger computational domain and the higher resolution of coastal features that may influence surge propagation along and across the coast. As a result, predictions from ADCIRC simulations may be more sensitive to storm characteristics, especially the storm surge response near fine-scale topographic features.

The ASGS was employed during Hurricane Arthur (2014), a Category 2 storm that impacted the North Carolina (NC) coastal region during early July 2014 (Berg, 2015). As the storm moved over Pamlico Sound (Fig. 1), it created storm surges up to 2.5 m, which pushed first into the river estuaries and against the inner banks, and then moved eastward to threaten the sound-side of the barrier islands. Early forecast advisories from the National Hurricane Center (NHC) predicted the storm to remain offshore. These forecast advisories also differed in their predictions of the storm's intensity. These track errors were not large in an absolute sense (about 130 km, which is less than the annual average track error for NHC predictions for the period 2010–2016 (National Hurricane Center, 2017)), but we hypothesize that their effects on flooding predictions were significant due to the nonlinear interactions of winds, waves and storm surge within the NC coastal system.

Recent studies have examined the sensitivity of storm surge

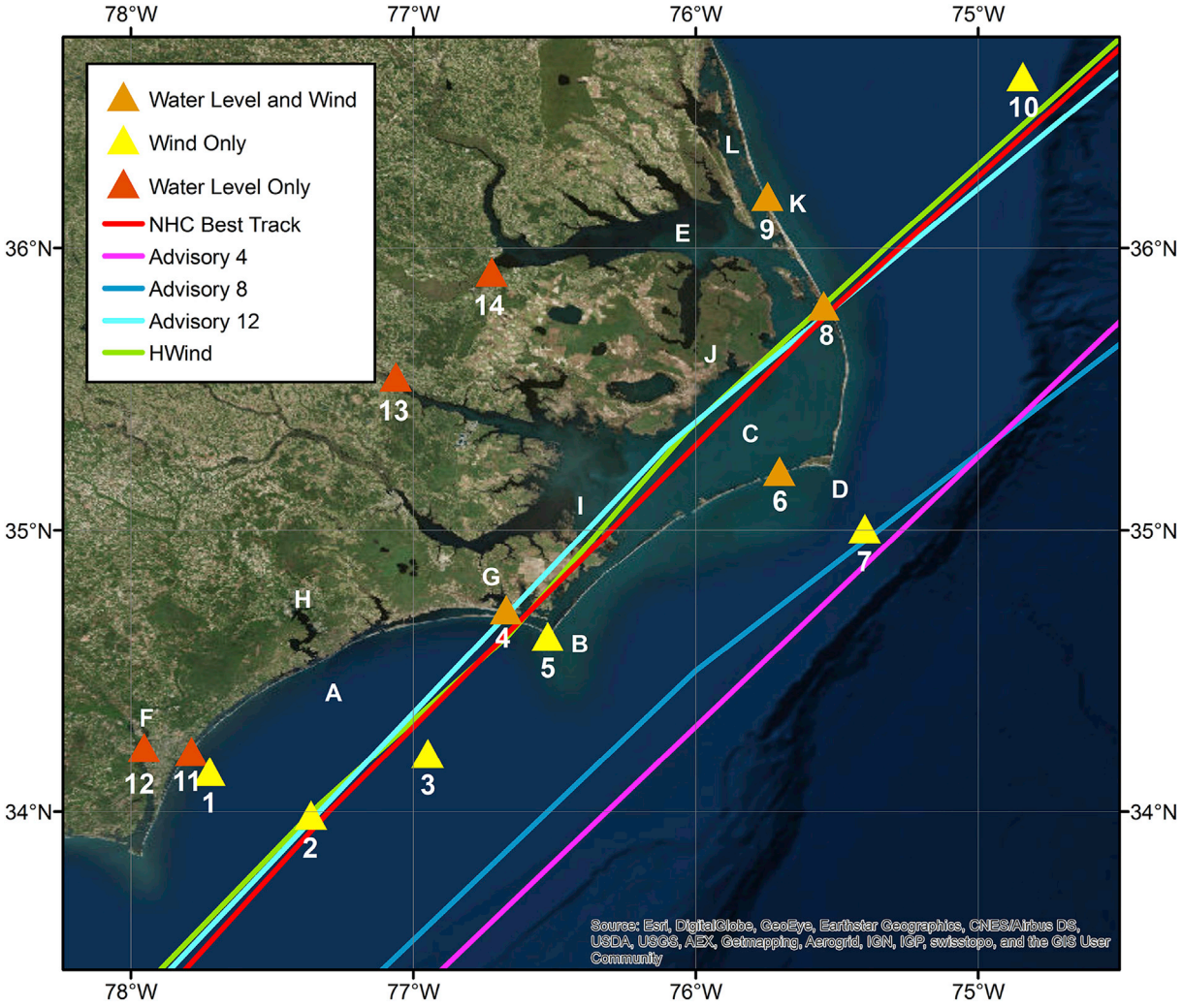

Fig. 1. Observation stations used for model validations (indicated by numbers) and other important geographic locations along the NC coast that are referenced in the paper (indicated by alphabets). Please refer to Table 1 for detailed description. Lines indicate storm track predictions during advisories 4 (pink), 8 (blue) and 12 (cyan) issued by the NHC 54, 30 and 12 h before Arthur made landfall along the NC coast. The best track (red line) issued after the storm by the NHC and the storm track represented by HWind (light green) is also shown. (For interpretation of the references to colour in this figure legend, the reader is referred to the Web version of this article.)

predictions to errors in forecast storm parameters. Site- and time-specific forecast uncertainties in storm parameters (storm intensity, size, forward speed and track angle) were estimated from archived historical storm data and applied to develop probabilistic surge estimates for synthetic storms at point locations inside New Orleans (Resio et al., 2017). For idealized storms over coastal NC, it was found that storm surge and inundation are sensitive to the forward speed, size, and track angle relative to the coast (Peng et al., 2004, 2006).

For Isabel (2003) in Chesapeake Bay, it was found that the storm surge magnitude and timing were sensitive to errors in the storm track, intensity, and forward speed, although the response varied spatially (Zhong et al., 2010). However, the above deterministic studies used hypothetical perturbations from either idealized storms or the best-track information, i.e., the storm track was shifted by 100 km, or the wind speed was increased or decreased by 50 percent. They did not consider the real uncertainties in storm information during the forecasts before landfall. For Isaac (2012) in Louisiana, the forecast performance of ADCIRC was evaluated for different sources of atmospheric forcing (Dietrich et al., 2012a), but the relative effects of storm parameters were not considered.

In this study, we analyze the performance of ADCIRC during Arthur, especially with respect to errors in the storm track forecasts from the NHC. Arthur provides a suitable opportunity for this analysis, because track forecasts evolved from a scenario without landfall (and minimal impact to coastal regions) to a scenario with the storm moving directly over Pamlico Sound, creating significant storm surge and flooding. The earlier forecast advisories from the NHC (e.g., advisory 4 issued 54 h before landfall) estimated that Arthur would follow an eastward track without making landfall along the NC coast, but these predictions changed progressively in advisories issued closer to landfall (Fig. 1). Advisory 12 (issued 6 h before landfall) was a close representation of the storm's true track over Pamlico Sound. However, even as the projected storm track was improving, the forecasts were projecting the storm to grow too powerful. Through comparisons with observed water levels during the storm, and with simulations forced by the best-track, post-storm guidance issued by the NHC, it is shown that the later surge predictions were a progressively-worse representation of the storm's impact on the surge environment in coastal NC. By isolating the effects of errors in storm track and storm strength, we will quantify the relative importance of these parameters in predicting peak wind speeds and storm surge. This knowledge will benefit real-time storm surge forecast systems to suitably incorporate the effects of errors in storm track and intensity while providing flooding predictions.

2. Hurricane Arthur (2014)

2.1. Synoptic history

Hurricane Arthur was the first named storm of the 2014 Atlantic hurricane season. It formed off the southeastern coast of United States and was classified as a tropical depression on 2014/07/01/0300 UTC (Berg, 2015), when the NHC issued its first forecast advisory. At 2014/07/01/1200 UTC, the depression developed into a tropical storm located about 111 km east of Ft. Pierce, FL. During the next three days, the storm moved northward and strengthened into a hurricane by 2014/07/03/0000 UTC, as it moved offshore of Savannah, GA. Arthur made landfall along the NC coast near Shackleford Banks at 2014/07/04/0315 UTC as a Category 2 hurricane on the Saffir-Simpson scale. The storm moved northeastward over Pamlico Sound, moved over the northern Outer Banks at 2014/07/04/0800 UTC, and then continued into the northern Atlantic Ocean (Berg, 2015).

The NHC forecasts changed significantly during the two days before Arthur's initial landfall in NC. For most of the forecast advisories, the storm was projected to remain offshore, with a track that moved northeastward off the Outer Banks. The forecast track shifted westward, and by advisory 10, the storm was projected to move over Cape Hatteras. By advisory 12, the projected landfall location was very close to the storm's initial landfall near Shackleford Banks, NC. This improvement in track forecast accuracy can be quantified via the error in storm center position (Fig. 3, left). These errors are computed as distances relative to the storm center in a data-assimilated wind product, which is described below, at 2014/07/04/0300 UTC, as the storm was making its initial landfall. For advisory 5, the storm center was in error by 137 km; by advisory 12, the storm center had corrected to within 9 km of the correct landfall location. Thus, the forecast track accuracy improved by about 3 km/hr (or 18 km per advisory) as Arthur approached NC.

During that same time, the storm was projected to increase in size and intensity. The storm's strength can be represented by the power dissipation (*PD*, (Emanuel, 2005)):

$$PD = \int_A C_D \rho \left|\mathbf{V}\right|^3 dA$$

in which C_D is the drag coefficient, ρ is the surface air density, $|\mathbf{V}|$ is the magnitude of the surface wind velocity, and the integral is evaluated over the surface area A of the storm. *PD* has units of energy per time, or power, with units of watts. Herein, we assume the linear drag coefficient relationship from (Garratt, 1977) with a maximum value of $C_D = 0.0035$, and assume a surface air density of 1 kg/m^3. For each of the atmospheric products described below, the integral will be computed over the entire computational domain, including any land masking used by the wave and circulation models; thus, the *PD* can be seen as a measure of the available power to the wave and circulation models. For the NHC forecast advisories, the *PD* increased generally as Arthur approached NC, from a value for advisory 4 of $2.04 \cdot 10^{12}$ watts, to a value for advisory 12 of $3.11 \cdot 10^{12}$ watts. Thus, as the forecast track was improving, the projected storm strength was increasing by more than 50 percent.

2.2. Observations

Arthur's effects in the coastal environment were captured by observations at: offshore buoys operated by the National Data Buoy Center (NDBC), Coastal Ocean Research and Monitoring Program (CORMP), and US Army Corps of Engineers; tide gauges operated by the National Ocean Service (NOS); and river gauges operated by the U.S. Geological Survey (USGS). These stations (described in Fig. 1 and Table 1) provide a valuable description of the evolution of wind speeds and surge levels as Arthur moved through coastal NC. Wind speeds measured at the NDBC

Table 1
Summary of station locations at which measurements of wind speeds and water levels are available for the study period.

Number	Longitude	Latitude	Station ID	Agency	Winds	Water Levels
1	−77.721	34.142	41038	CORMP	X	
2	−77.363	33.988	41037	CORMP	X	
3	−76.949	34.207	41036	NDBC	X	
4	−76.667	34.716	BFTN7/ 8656483	NOAA/ NOS	X	X
5	−76.525	34.622	CLKN7	NOAA/ NOS	X	
6	−75.704	35.209	HCGN7/ 8654467	NOAA/ NOS	X	X
7	−75.402	35.006	41025	NDBC	X	
8	−75.548	35.796	ORIN7/ 8652587	NOAA/ NOS	X	X
9	−75.746	36.184	DUKN7/ 8651370	NOAA/ NOS	X	X
10	−74.842	36.61	44014	USACE	X	
11	−77.786	34.213	8658163	NOAA/ NOS		X
12	−77.9533	34.2267	8658120	NOAA/ NOS		X
13	−77.062	35.543	2084472	USGS		X
14	−76.723	35.915	208114150	USGS		X

offshore buoys and land stations are processed to match the 10-min averaging period of ADCIRC wind speeds. The averaging periods for the measurement data are 8-min for buoys (41036, 41037 and 41025) and 2-min for land stations (BFTN7, HCGN7, ORIN7, DUKN7 and CLKN7). Using site-specific inputs such as terrain roughness and Coriolis parameter, the measurement data are referenced to 1-hr mean wind speeds, and then gust factors are computed for the conversion to 10-min wind speeds ((Vickery and Skerlj, 2005)). Based on an analysis at station ORIN7, a factor of 1.076 is used to convert the observations to 10-min wind speeds at all the land stations. A similar analysis yielded a conversion factor of 1.005 for observations at the NDBC buoys (41037 and 41025).

3. Methods

3.1. Models for storm-induced waves and surge

The hyrdrodynamic model ADCIRC (adcirc.org) solves modified forms of the shallow water equations. It uses the Generalized Wave Continuity Equation (GWCE) for water levels and either the three-dimensional or the vertically integrated momentum equations for currents U and V ((Luettich and Westerink, 2004; Dietrich et al., 2012b; Dawson et al., 2006; Murty et al., 2014; Bhaskaran et al., 2013)). The evolution of waves is simulated using SWAN (Simulating WAves Nearshore), a phase-averaged wave model that describes the evolution of action density N (t, λ, ϕ, θ, σ) in time (t), geographic space (with longitudes λ and latitudes ϕ) and spectral space (with directions θ and frequencies σ). During tightly coupled ADCIRC+SWAN simulations, wind speeds, water level, current velocities and roughness lengths provided by ADCIRC are used by SWAN to calculate the radiation stress gradients responsible for the wave-induced setup that contributes to water levels ((Dietrich et al., 2011, 2012b; Hope et al., 2008)). For the present study, ADCIRC simulations are performed with a time step of 0.5 s, while the SWAN time step and coupling interval are 1200 s. Spatially-variable settings are used for the weighting factor (τ_0) in GWCE (0.005 in open water, 0.03 inland), eddy viscosity ($2m^2/s$ in open water, and 10 m^2/s inland), and Mannings n (default value of 0.02 in open water, with larger inland values based on land-cover).

3.2. Atmospheric forcing

We utilize two sources of atmospheric forcing: an analysis product based on observations, and a parametric vortex model based on storm parameters from the NHC guidance.

3.2.1. Real-time hurricane wind analysis system (HWind)

Spatially- and temporally-varying wind fields can be constructed from observations of wind velocities during a storm. The Real-Time Hurricane Wind Analysis System (HWind) was developed as part of the NOAA Hurricane Research Division (Powell et al., 1998). Observations of wind velocity relative to the storm center are incorporated by HWind, which converts them to a common reference frame at 10-m height, peak 1-min-averaged sustained wind speed, and marine exposure. Wind velocities from airborne stepped-frequency microwave radiometers, GPS dropsondes, buoys, ships, satellite-based visual imagery, and land-based platforms (DiNapoli et al., 2012) are then smoothed and interpolated onto a regular grid by minimizing the least-square differences between observations and analysis (Powell et al., 1996). Starting with the 2013 hurricane season, these wind fields have been produced by Risk Management Solutions, Inc. (RMS, http://www.rms.com/perils/hwind/). These wind fields are developed with observations during the storm, and thus can be used only for hindcasting.

The HWind fields for Arthur are available for 3.625 days from 1800 UTC on 1 July 2014 through 0900 UTC on 5 July 2014. The gridded HWind field is interpolated spatially onto ADCIRC mesh vertices at every available snap of HWind data, and then interpolated temporally to derive the wind field for intermediate time steps. The storm vortex structure is preserved by utilizing HWind data snaps that are spaced closely in time (every 3 h during the peak of the storm). The wind speeds are converted from a 1-min sustained wind speed to a 10-min wind speed for use by ADCIRC, by using a multiplier of 0.893 (Powell et al., 1996). The HWind fields do not include surface pressures, so central pressures from the NHC Best-Track guidance were used to generate pressure fields in space and time. This method uses the Holland vortex model (Holland, 1980) to compute barometric pressure with distance from the storm center.

3.2.2. Generalized Asymmetric Holland Model (GAHM)

When ADCIRC is used for real-time storm surge forecasting during tropical cyclones, it constructs pressure and wind fields within its computational domain by using a parametric vortex model based on (Holland, 1980). Axisymmetric pressure and wind fields can be computed from a limited set of parameters such as the storm's eye location, central pressure, radius to maximum winds (RMW), and maximum sustained wind speed, all of which are available in the advisories issued by the NHC. This model has been modified to reflect storm asymmetry with an azimuthally-varying RMW, by using the distance to the highest-specified isotach in each of the storm quadrants (Xie et al., 2006). This parametric vortex model, which do not include the background wind field, has been used as atmospheric forcing to generate storm surge predictions for previous storms (Luettich and Westerink, 2004; Mattocks and Forbes, 2008; Forbes et al., 2010; Dietrich et al., 2013b).

In this study, we utilize a newer version of the parametric vortex model that removes the assumption of cyclostrophic balance at the location of the maximum wind speed around the storm and also allows the use of multiple isotachs in each wind quadrant to better specify the storm wind field. The cyclostrophic assumption (i.e., neglecting the Coriolis force) at RMW is valid for strong and compact TCs, but it introduces errors for generally weak or large TCs, or TCs at their developing or dissipating stages. The Generalized Asymmetric Holland Model (GAHM) has been developed to avoid these assumptions. The assumption of cyclostrophic balance is eliminated, and multiple isotachs are used to construct the wind field, thus ensuring that modeled winds match all available information. GAHM has been shown to be a better representation of the storm, via comparisons of model results for past hurricanes with the corresponding best-track guidance, e.g., for Hurricane Isaac (2012) in southeastern Louisiana (Dietrich et al., 2012a).

GAHM is integrated within the ADCIRC source code and uses information from NHC advisories in the Automated Tropical Cyclone Forecast (ATCF) format. It requires parameters about the wind field: maximum sustained wind speed (column 9 in the ATCF format), wind intensities for the identified isotachs (column 12), radii to the isotachs (columns 14–17), and RMW (column 20). It also requires information about the pressure field: minimum sea level pressure (column 10), and background pressure (column 18). The file containing this information is pre-processed to add columns with quadrant-specific values for RMW, maximum wind speed, and the Holland B parameter.

3.3. Swapping information between HWind and GAHM

The studies below consider scenarios in which these two atmospheric forcings are mixed, i.e., storm parameters from the HWind analysis are applied in GAHM. The reasoning for this mixture of storm parameters is discussed in the sections below; for now, we describe how we move storm information between the two forcings.

To examine the affects of errors associated with storm track, one set of scenarios replaces the storm strength parameters from the NHC forecast guidance with the same parameters derived from post storm analysis. For the wind field, the isotach values are replaced with wind speeds and radii interpolated from isotachs in the gridded HWind fields. For example, to find the radii to the 34-knot isotach, we move outward in the HWind field in each quadrant until we find the grid cell containing the isotach, and then use a linear interpolation to find its distance from the storm center.

For the pressure field, the values are replaced with information from the NHC best-track guidance, because the HWind analysis does not provide information about the pressure fields. Values are replaced in the appropriate columns in the ATCF-formatted files for use with GAHM. In this way, the storm intensity and size are unchanged, but the storm track varies with each advisory.

To examine the effects of errors associated with storm strength, another set of scenarios replaces the track in the NHC forecast guidance with the track extracted from the HWind analysis. The storm center positions are identified in the HWind gridded files, and then used to adjust the values used with GAHM. For example, to adjust the track for the wind- and pressure-fields corresponding to 2014/07/02/0000 UTC, we find the storm center position from the HWind gridded file for that date and time, and then use it to replace the position in the corresponding entry in the ATCF-formatted file. This process is repeated for the other dates and times during the simulation. In this way, the storm track is unchanged, but the storm strength parameters (that determine the wind- and pressure-fields) vary with each advisory.

3.4. Unstructured mesh describing coastal NC

The unstructured, finite-element mesh used in the present study is NC v9.98 (referred to as the NC9 mesh throughout this study), which covers the entire Western North Atlantic, the Gulf of Mexico and the Caribbean Sea. Such a large domain for ADCIRC helps to minimize errors associated with open ocean boundary conditions and to track hurricane movement throughout the domain ((Dresback et al., 2011)). The mesh extends inland along the NC coast to the 15-m topographic contour to allow for storm surge flooding (Fig. 2). In this region, the mesh has been designed to resolve bathymetric and topographic features such as inlets, dunes and rivers as identifiable on satellite images, NOAA charts, shoreline datasets and high-resolution DEMs with data from multiple sources ((Blanton et al., 2008)). This mesh includes sufficient resolution to represent realistically the numerous inlets through the NC barrier islands, the back bays and sounds, and the Atlantic Intracoastal Waterway that runs north-south through the NC sounds (Blanton and Luettich, 2008; Blanton et al., 2012b) There are a total of 622,946 computational vertices and 1, 230,430 elements in the NC mesh; more than 90 percent of this resolution is applied within coastal NC. Large elements with a mesh spacing of 50 to 100 km describe the Gulf of Mexico and open Atlantic, and the elements decrease in size as the bathymetry transitions to near-shore conditions. Mesh spacing along the NC coastline varies from 3 to 4 km on the continental shelf to about 100 m near the Outer Banks. Resolution in Pamlico and Albemarle Sounds is 1500 to 1800 m in the deeper regions and, reduces to 100 to 300 m at the entrance of the river channels and in the shallower regions that border the sounds. Resolution of the narrow river channels that extend inland from the sounds and elsewhere along the NC coastline is generally less than 50 m. The topography/bathymetry values have NAVD88 as their vertical datum and NAD83 as the horizontal datum.

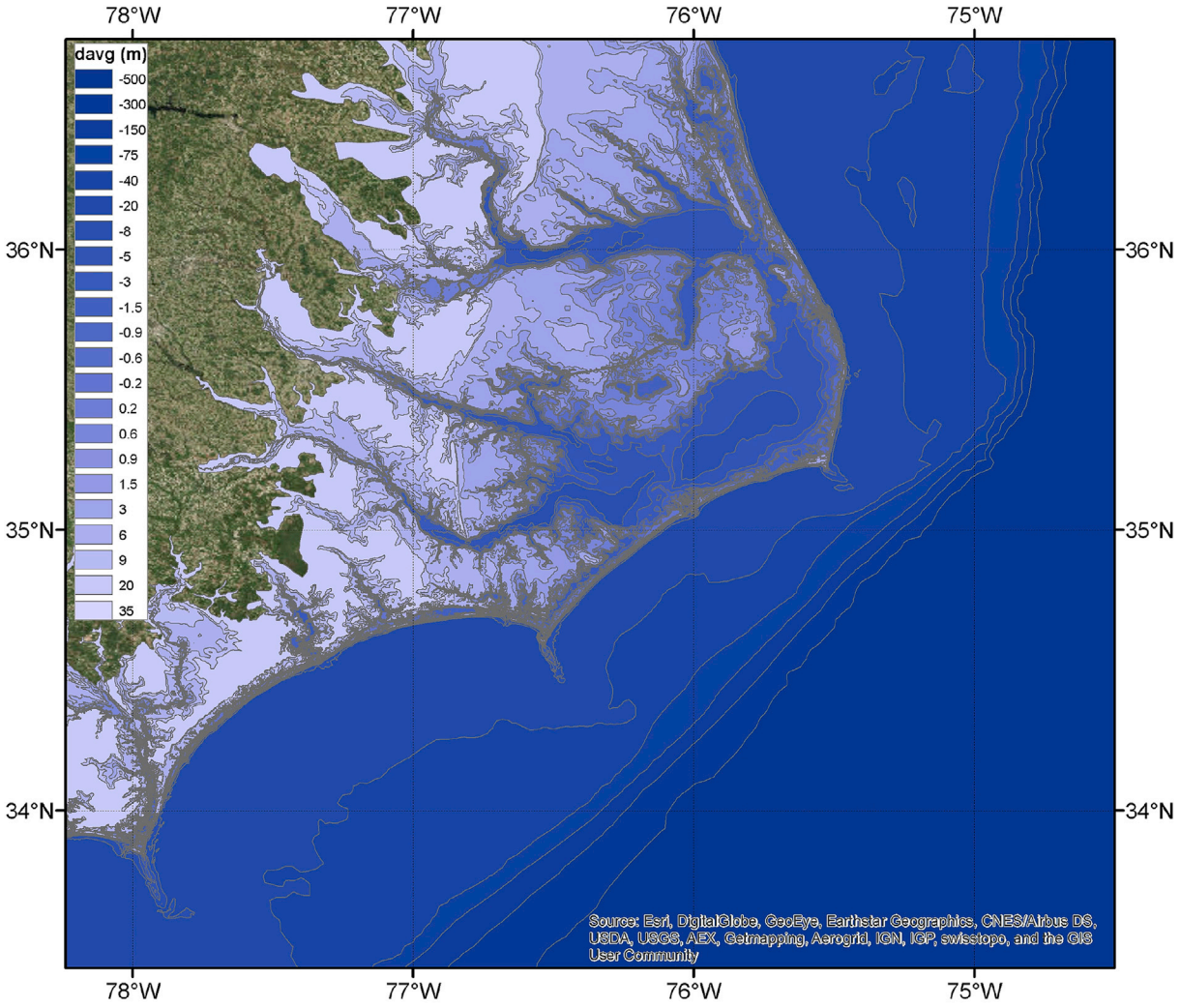

Fig. 2. Bathymetry and topography contours (m, relative to mean sea level) for the NC9 mesh used by the ASGS for generating storm surge forecasts during Hurricane Arthur (2014).

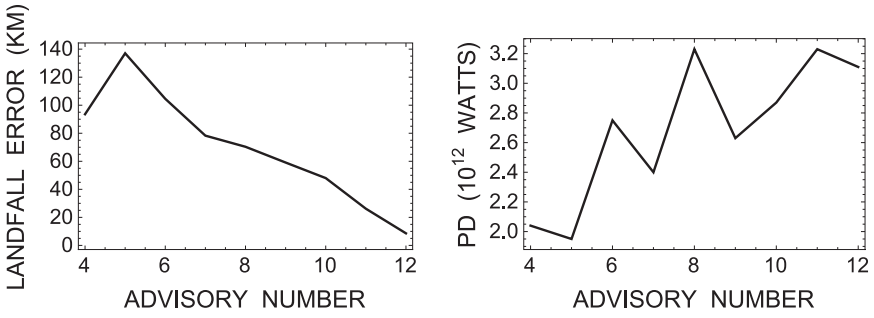

Fig. 3. Evolution by forecast advisory number of Arthur's (left) forecast landfall error (km) at 2014/07/04/0300 UTC, and (right) power dissipation (10^{12} watts) averaged over 24 hr surrounding its initial landfall.

4. Results and discussion

4.1. Validation for atmospheric products available before and after the storm

4.1.1. Hindcasts

To understand the true effects of Arthur on coastal North Carolina, we consider the best-available representations of Arthur from two atmospheric forcings: the HWind analysis product, and GAHM using the Best-Track guidance for storm parameters issued by the NHC. We denote the first simulation as *HWind*, and the second simulation as *GAHM(BT)*. Also, to examine GAHM's ability to reproduce the wind field described by HWind, we consider a third simulation with a hybrid of forcings: GAHM using the track and wind-field parameters from HWind, denoted as *GAHM(HWind)*. The sources of tracks, wind- and pressure-fields for all simulations are summarized in Table 3.

Winds – The hindcasts represent the observed path of Arthur as it made landfall, passed over Pamlico Sound, and then followed a northeastward track away from the coast. At 2014/07/04/0000 UTC, Arthur was positioned in Onslow Bay and was moving toward the shore with mean wind speeds greater than 35 m/s. The eye was positioned southeast of Wilmington, and the storm had mean wind speeds of 25 – 30 m/s to the south of Beaufort, NC. (Geographic locations of specific cities, bays, sounds, etc. are summarized in Fig. 1 and Table 2) Three hours later at 2014/07/04/0300 UTC, Arthur made its first landfall at Shackleford Banks near Beaufort, NC, as a category 2 storm with mean wind speeds between 35 – 40 m/s along the coast from Jacksonville to Cedar Island, NC (Berg, 2015). Further north, the mean wind speeds were larger than 25 m/s over Pamlico Sound behind the barrier islands. The winds were beginning to blow southeasterly over this region because of the storm's northeastern trajectory.

By 2014/07/04/0600 UTC, Arthur made a second landfall near Hyde County, NC, as the storm moved over Pamlico Sound. This landfall was accompanied by northwesterly winds with mean speeds as large as 37 m/s blowing over Pamlico Sound and adjacent regions. The *HWind* and *GAHM(BT)* simulations are a good match in the storm track and forward speed, and are a decent match for the peak wind speed, but are different in the size of the storm. This behavior can be observed in the predictions as the storm was moving over Pamlico Sound (Fig. 4, left column). For *HWind*, the peak wind speeds (larger than 30 m/s) are contained within the southeast quadrant of the storm, while for *GAHM(BT)*, these peak winds extend into the southwest and northeast quadrants, thus affecting regions along the track of the storm. In the Neuse and Pamlico River estuaries on the west end of Pamlico Sound, and also within Albemarle Sound to the north, the wind speeds are about 5 m/s larger in *GAHM(BT)* than in *HWind*. These trends are repeated in the maximum wind fields experienced during the storm (Fig. 4, center and right columns). The *GAHM(BT)* wind speeds are about 10 m/s larger along the storm track, but the difference is smaller to the east of the track, where the peak winds occurred during the storm. Using the NHC best-track storm parameters, *GAHM(BT)* is producing a storm with the correct track and peak intensity, but that is too large.

When GAHM is applied with the storm track and wind information from HWind, the *GAHM(HWind)* simulation is a better match to the size of the storm (Fig. 4, bottom row). The peak wind speeds are contained within the southeast quadrant, although rotated southward relative to *HWind*. The maximum wind speeds are still too large in *GAHM(HWind)* by about 5 – 8 m/s along the storm track, but there is a significant improvement relative to *GAHM(BT)*. Given a similar set of storm parameters, *GAHM(HWind)* matches well to the wind field in the HWind analysis product.

The observations reveal similar behavior (Fig. 5). While *HWind*, whose wind forcing is most realistic due to post storm data assimilation, is generally a good match to the observations, including at the storm peak, *GAHM(BT)* has wind speeds that are generally too large by 5 – 10 m/s, including both before and at the storm peak. At the NDBC stations 41037 and BFTN7, the peak wind speed is overpredicted by *HWind*

Table 2
Summary of selected locations along the North Carolina coast referenced in the text.

Code	Location
A	Onslow Bay
B	Cape Lookout
C	Pamlico Sound
D	Cape Hatteras
E	Albemarle Sound
F	Wilmington
G	Beaufort
H	Jacksonville
I	Cedar Island
J	Hyde County
K	Kitty Hawk Island

Table 3
Summary of storm tracks, wind and pressure fields used in each simulation. Each forecast simulation uses information from the corresponding NHC forecast advisory, e.g., *GAHM(4)* uses parameters from NHC forecast advisory 4 to construct wind and pressure fields using GAHM. For hybrid simulations, the track and storm information comes from different sources, e.g., *GAHM(12,HWind)* uses the storm track from NHC forecast advisory 12, but with parameters for storm size and intensity from the hindcast *HWind* simulation.

Type	Simulation	Track	Wind	Pressure
Hindcast	*HWind*	HWind	HWind	NHC BT
	GAHM(BT)	NHC BT	NHC BT	NHC BT
	GAHM(HWind)	HWind	HWind	NHC BT
Forecast	*GAHM(4–12)*	NHC 4-12	NHC 4-12	NHC 4-12
Track Uncertainty	*GAHM(4–12,HWind)*	NHC 4-12	HWind	NHC BT
Storm Uncertainty	*GAHM(HWind,4–12)*	HWind	NHC 4-12	NHC 4-12

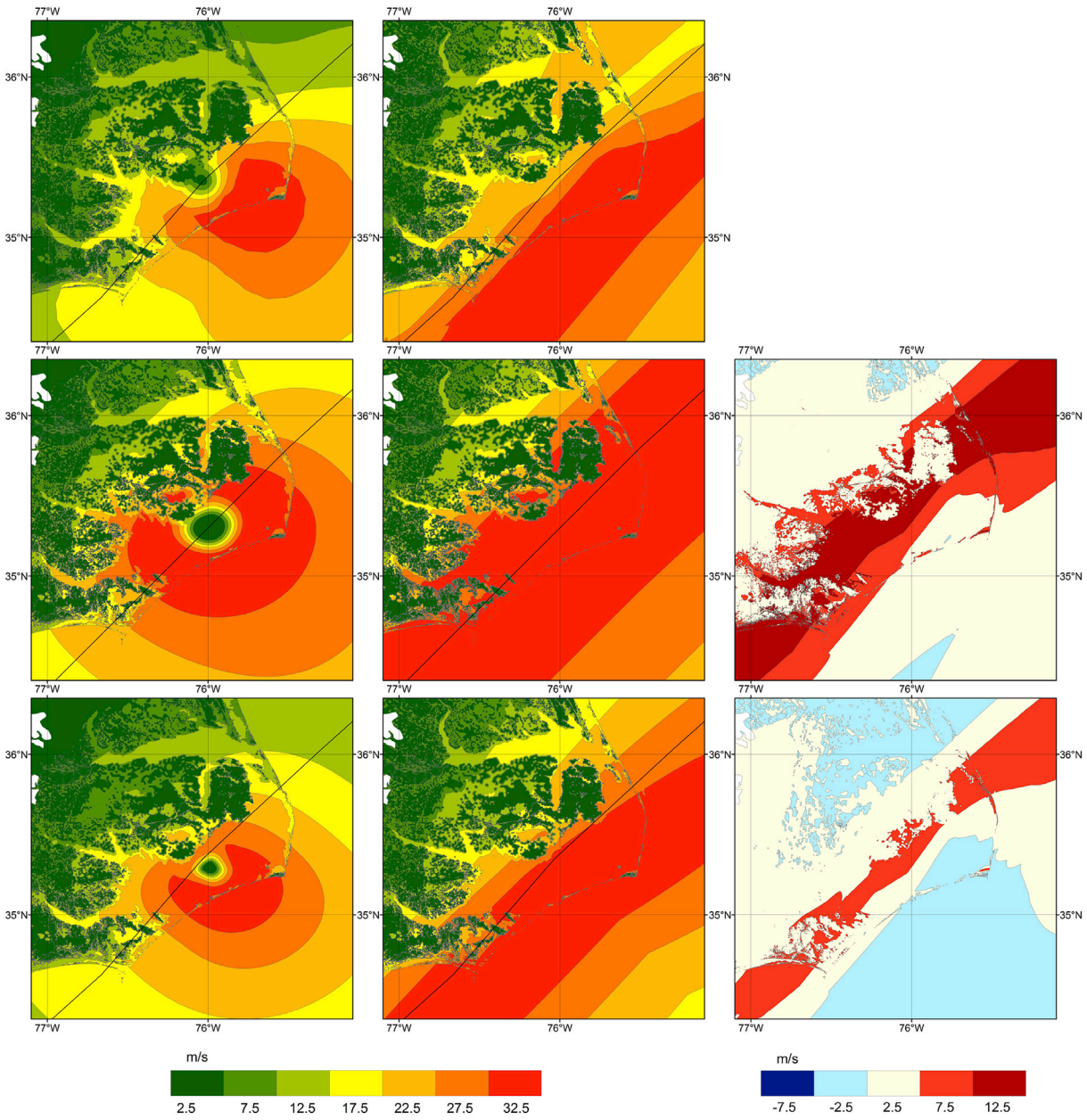

Fig. 4. Hindcasts of wind speeds (m/s) during Arthur in coastal North Carolina. Rows correspond to: (top) *HWind*, (middle) *GAHM(BT)*, and (bottom) *GAHM(HWind)*. Columns correspond to: (left) wind speeds at 2014/07/04/0600 UTC, (center) maximum wind speeds, and (right) difference in maximum wind speeds relative to *HWind*.

as above 34 m/s, when the observed peaks are less than 30 m/s at these locations. At stations farther east, such as the stations at Oregon Inlet and Duck, the observed peaks were between 24 – 27 m/s, but *GAHM(BT)* overpredicts by as much as 8 m/s. Many of these errors are corrected in *GAHM(HWind)*, which has wind speeds that are a better match to the peak winds. The model predictions are compared to observations using statistical measures including mean normalized bias (B_{MN}, which is a measure of the model's magnitude of over- or under-prediction normalized to the observed value, with an ideal value of zero):

$$B_{MN} = \frac{\frac{1}{N}\sum_{i=1}^{N} E_i}{\frac{1}{N}\sum_{i=1}^{N} |O_i|}$$

and root-mean-squared difference (*RMS*, which is a measure of the magnitude of the error, with an ideal value of zero):

$$RMS = \sqrt{\frac{1}{N}\sum_{i=1}^{N} E_i^2}$$

where O is the observed value, E is the error in terms of model minus observed, and N is the number of observations (or computational points, for later comparisons). For these 10 stations with observations of wind speeds, the *RMS* difference is nearly doubled from 2.69 m/s for *HWind* to 4.63 m/s for *GAHM(BT)*, but it is lowered to 3.79 m/s for *GAHM(HWind)* (Table 4). All three hindcasts show a slightly negative B_{MN} ranging from −0.05 for *GAHM(BT)* to −0.17 for *GAHM(HWind)*. It is noted that *GAHM(HWind)* does not contain the background wind and pressure fields, and thus it cannot represent the wind speeds of 6 – 8 m/s before and after the storm (such as those during the first 12 hr of Fig. 5). The negative bias values for *GAHM(BT)* and *GAHM(HWind)* reflect the

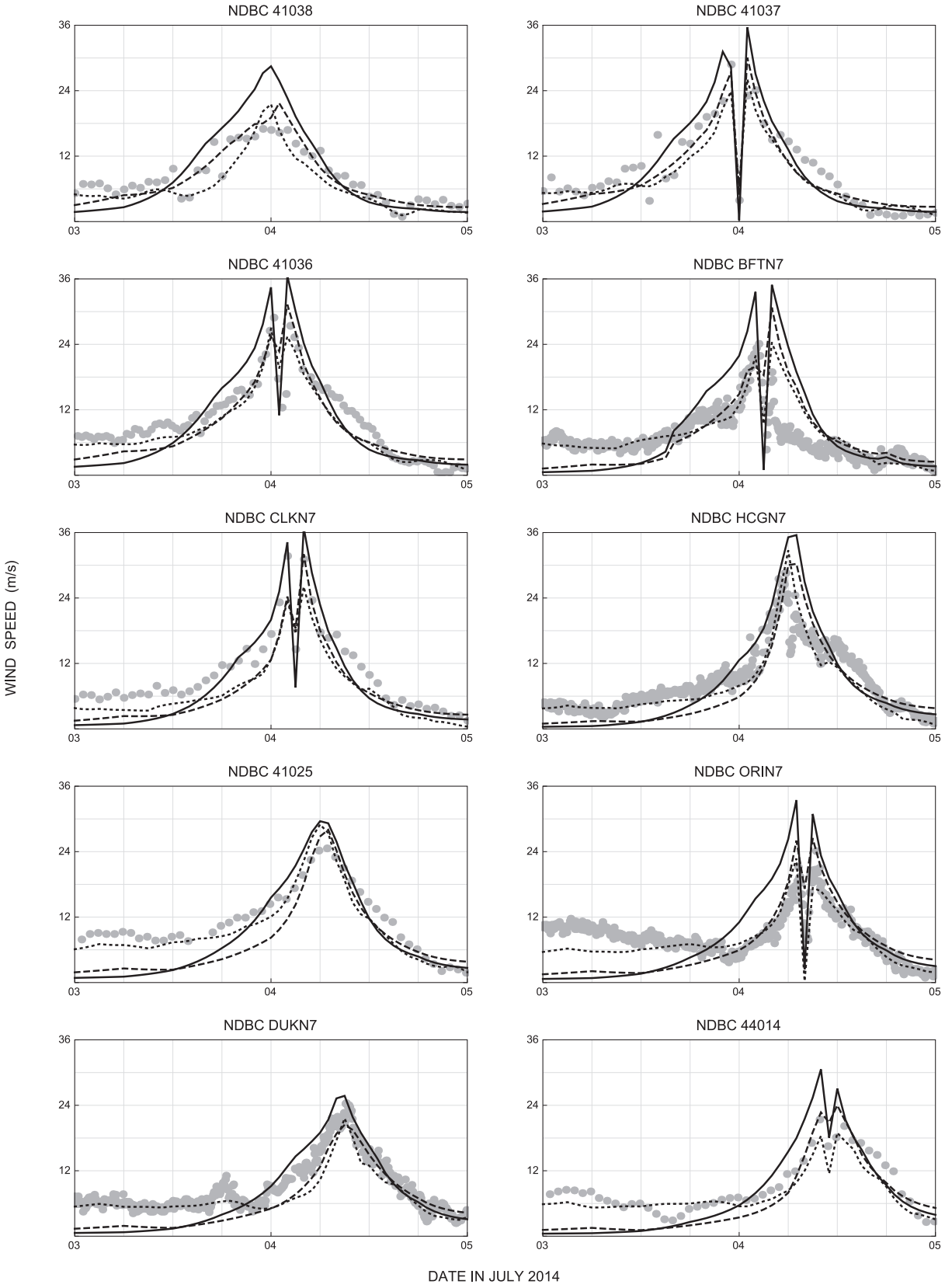

Fig. 5. Time series of observed and predicted wind speeds (m/s) from hindcast simulations at 10 stations with locations described in Table 1 and Fig. 1. Gray circles indicate observations, and the lines indicate predictions from (dotted) *HWind*, (solid) *GAHM(BT)*, and (dashed) *GAHM(HWind)*.

Table 4
Error statistics for the three hindcast simulations, for both wind speeds and water levels, with comparisons to the available observations in the region, and at every computational point with depths less than 10 m.

Simulation	Comparison to Observations				Comparison to *HWind*			
	Wind Speeds		Water Levels		Wind Speeds		Water Levels	
	B_{MN}	*RMS*	B_{MN}	*RMS*	B_{MN}	*RMS*	B_{MN}	*RMS*
HWind	− 0.12	2.69	− 0.17	0.16				
GAHM(BT)	− 0.05	4.63	− 0.03	0.19	0.38	5.90	0.24	0.30
GAHM(HWind)	− 0.17	3.79	− 0.20	0.17	0.08	2.47	0.00	0.13

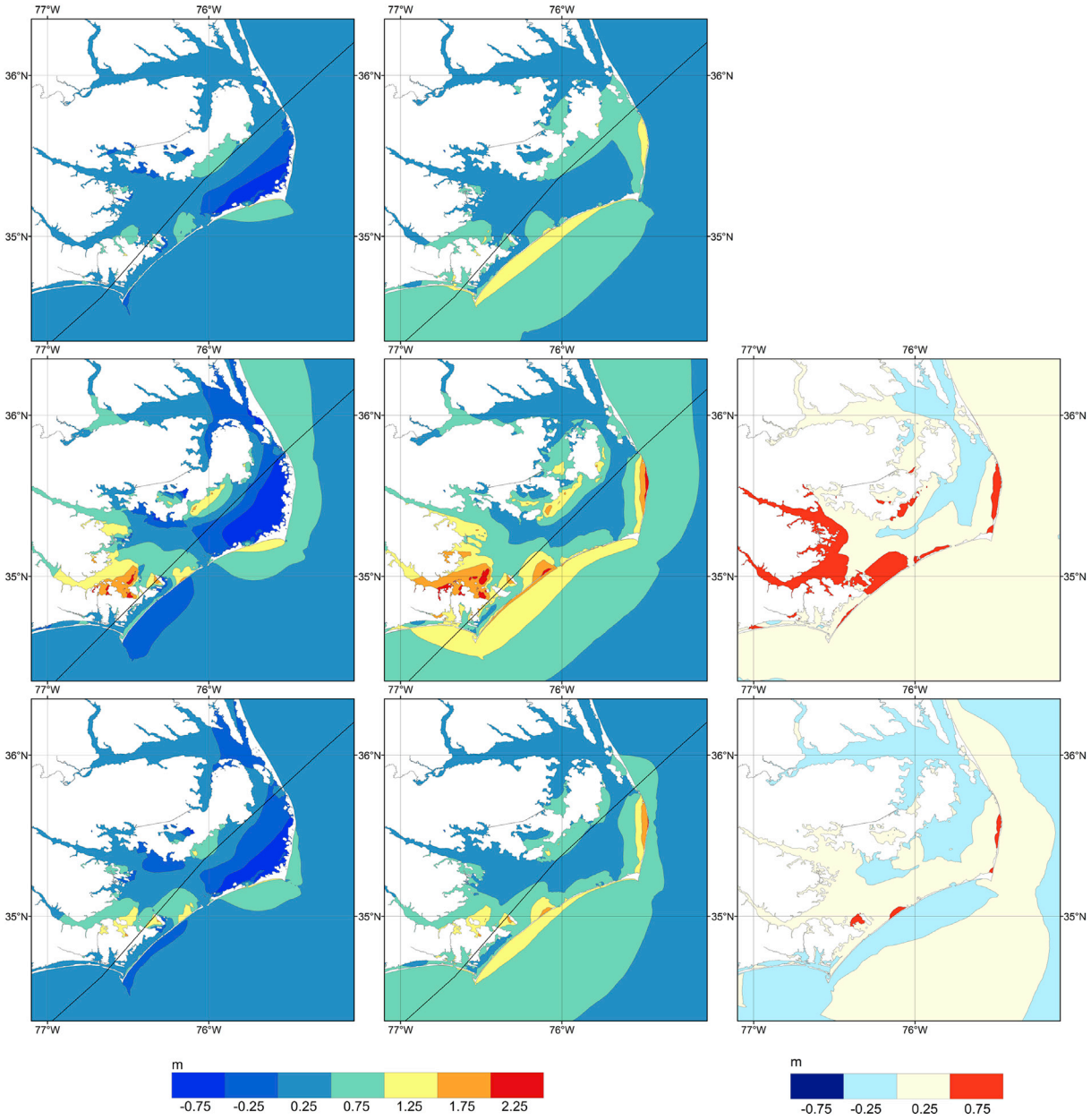

Fig. 6. Hindcasts of water levels (m) during Arthur in coastal North Carolina. Rows correspond to: (top) *HWind*, (middle) *GAHM(BT)*, and (bottom) *GAHM(HWind)*. Columns correspond to: (left) water levels at 2014/07/04/0600 UTC, (center) maximum water levels, and (right) difference in maximum water levels relative to *HWind*.

combined effect of the under prediction of observed wind speeds prior to the storm and over estimation at the peak. HWind is a post-storm, data assimilated wind product and is expected to provide a more accurate representation of Arthur compared to parametric vortex models that utilize limited storm information. The *HWind* errors can therefore be seen as a baseline, to which the GAHM simulations can be compared in later sections.*Water Levels* – Arthur had a significant effect on water levels throughout coastal NC, particularly by the generation of storm surge within the shallow sounds. At 2014/07/04/0000 UTC as the storm was still offshore, the water levels were increased by less than 0.5 m along the

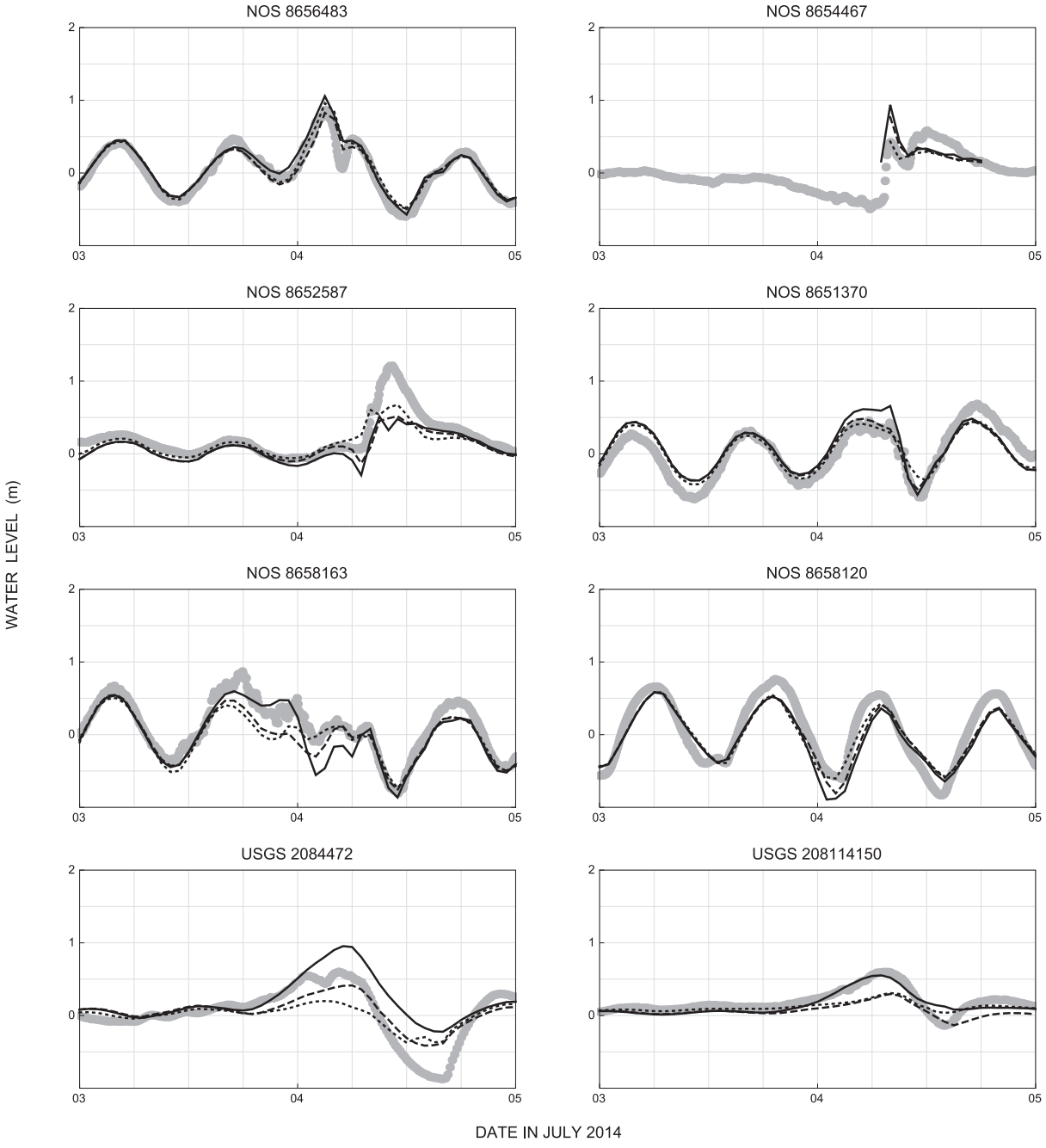

Fig. 7. Time series of observed and predicted water levels (m) from hindcast simulations at 8 stations with locations described in Table 1 and Fig. 1. Gray circles indicate observations, and the lines indicate predictions from (dotted) *HWind*, (solid) *GAHM(BT)*, and (dashed) *GAHM(HWind)*.

NC coast and in Pamlico and Albemarle Sounds. Three hours later, as the storm made its initial landfall at 2014/07/04/0300 UTC, the water levels had increased along the barrier islands to the south of Hatteras Island near Cape Lookout, NC. Wind and wave forcing were primarily responsible for this surge. At this time, the water levels were between 1 – 1.5 m where the storm made its first landfall near Beaufort, NC, and between 0.5 – 1.25 m in the Neuse and Pamlico Rivers extending inland from Pamlico Sound.

By 2014/07/04/0600 UTC, the eye of the storm was centered over Pamlico Sound (Fig. 6, left column), and water was pushed away from the Outer Banks creating storm surges between 0.5 – 1.75 m in the bays and channels extending from the northern parts of Pamlico Sound. Storm surge between 1.5 – 2 m also existed in the rivers and channels (Neuse and Pamlico River) along the southern and shallower parts of Pamlico Sound. There is significant variability in the water level predictions, both at this time and in the maxima during the storm (Fig. 6, left and center columns). *HWind* predicts peak water levels of about 1.5 m along the ocean-side of the barrier islands between Capes Lookout and Hatteras, and along the sound-side of Hatteras Island north of its cape. In *GAHM(BT)*, these peaks are increased to more than 2 m, and additional flooding is experienced along the Neuse River estuary. The peak water levels in *GAHM(BT)* are higher than in *HWind* by almost 0.5 m along the barrier islands, and by more than 1 m in the estuaries on the west side of Pamlico Sound. These differences are decreased for *GAHM(HWind)* due to its improved representation of the wind fields.

The storm's effects on the shallow waters along the NC coast are evident in a comparison to observations at six locations described in Fig. 1 and Table 1. At NOS station 8656483 (Beaufort), which is located

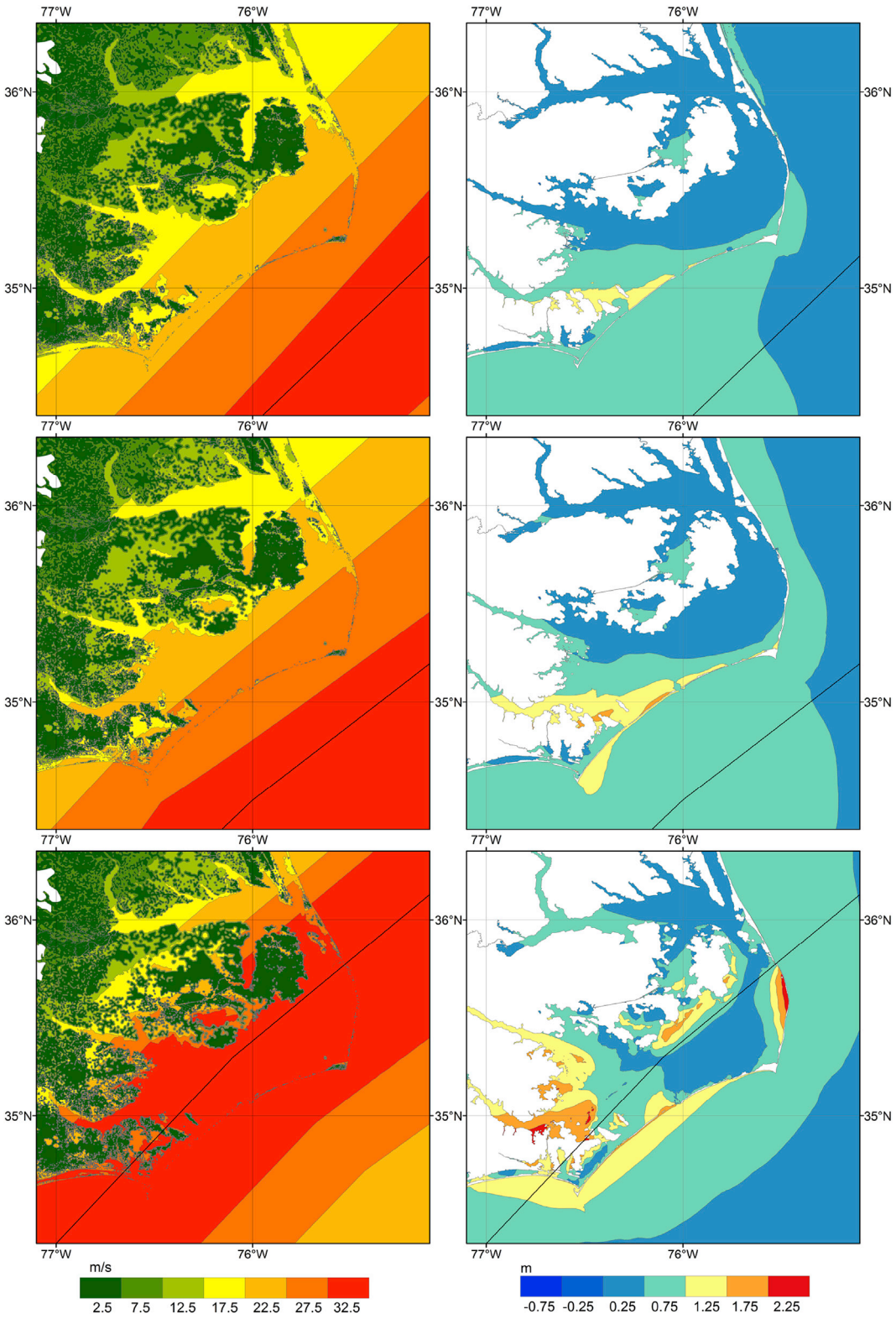

Fig. 8. Forecasts of winds (m/s) and water levels (m) during Arthur in coastal North Carolina. Rows correspond to: (top) *GAHM(4)*, (middle) *GAHM(8)*, and (bottom) *GAHM(12)*. Columns correspond to: (left) maximum wind speeds, and (right) maximum water levels.

near the path of the storm, the water levels predicted by the model using the best-track information agree well with the observations (Fig. 7). The northeasterly winds blowing over coastal NC created a storm surge, which matches within 0.2 m of the peak for all three hindcasts. At NOS station 8652587 (Oregon Inlet Marina), *GAHM(BT)* predicted a pre-peak drawdown of 0.3 m, while *HWind* showed rising water levels as the storm approached this location. The USGS stations are representative of locations farther inland in the river channels extending from the sounds. At USGS station 02084472 (Pamlico River), the observed peak water level of 0.6 m is bracketed by the model predictions, with *HWind* too low, and *GAHM(BT)* too high. At USGS station 0208114150 (Roanoke River), the observed peak water level is matched well by *GAHM(BT)*, but *HWind* is

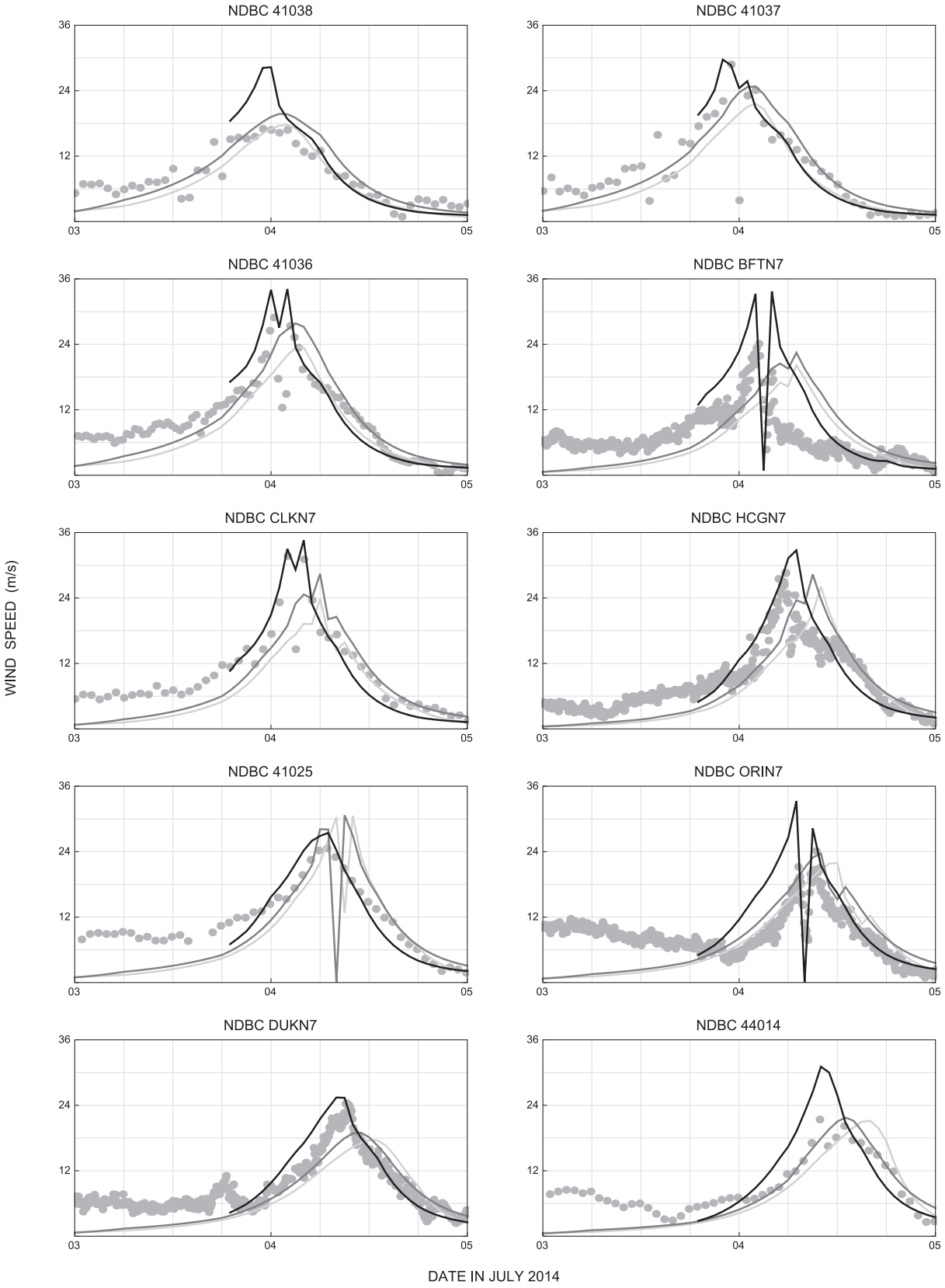

Fig. 9. Time series of observed and predicted wind speeds (m/s) from forecast simulations at 10 stations with locations described in Table 1 and Fig. 1. Gray circles indicate observations, and the lines indicate predictions for (lighter gray) *GAHM(4)*, (darker gray) *GAHM(8)*, and (black) *GAHM(12)*.

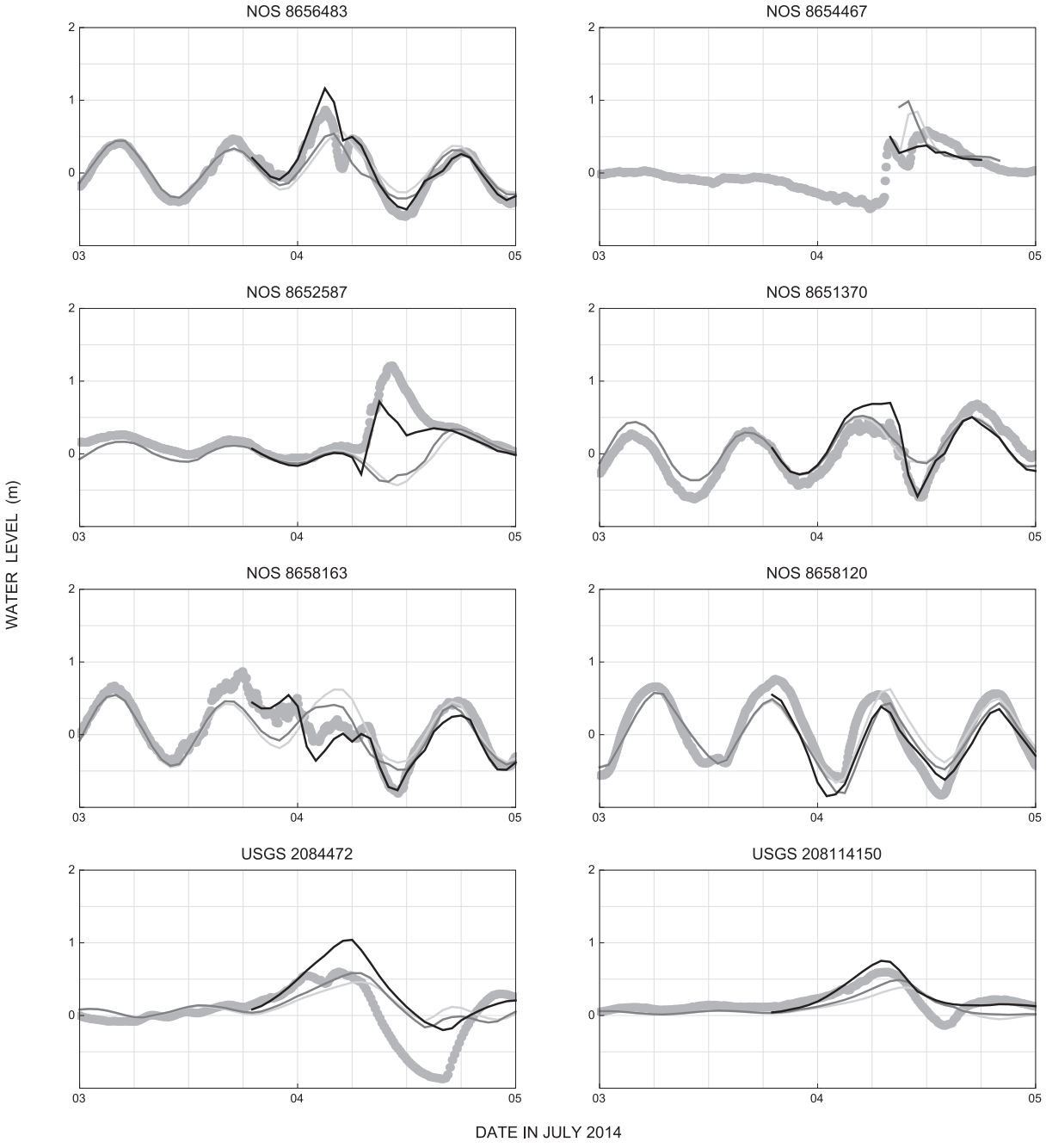

Fig. 10. Time series of observed and predicted water levels (m) from forecast simulations at 8 stations with locations described in Table 1 and Fig. 1. Gray circles indicate observations, and the lines indicate predictions for (lighter gray) *GAHM(4)*, (darker gray) *GAHM(8)*, and (black) *GAHM(12)*.

too low by 0.3 m. At NOS station 8651370 (Duck Pier), which is located to the east of Currituck Sound on the open Atlantic coast and farthest to the north (among all the stations), the storm does not cause an observable change from the tidal cycle, but the overestimated winds in *GAHM(BT)* cause the peak water levels to be overpredicted by 0.1 – 0.2 m.

Error statistics are computed for modeled and observed water levels at 8 observation stations (Table 4). The *RMS* differences are between 0.16 – 0.19 m for the three hindcasts, indicating a generally-good match between the predictions and the observations. However, these errors are highly dependent on station location relative to the storm track. To better represent the spatial distribution of errors in the region, the B_{MN} and *RMS* differences were computed for peak water levels between *HWind* and the GAHM hindcasts at every computational point (mesh vertex) with depth less than 10 m (similar to the analysis in (Forbes et al., 2010)). Relative to the *HWind* simulation, the *GAHM(BT)* peak water levels were too high, with a positive bias of 0.24 m and a root-mean-square error of 0.30 m in the region. The relatively-good bias for *GAHM(BT)* simulation reflects model performance over a full simulation. Water levels were over-predicted during the storm, the resulting positive bias is offset to a certain degree by the underprediction prior to the storm due to the absence of background winds. When the HWind storm parameters were used to construct the vortex wind field in GAHM, the *GAHM(HWind)* peak water levels were a close match, with a bias near zero and a root-mean-square error of 0.13 m. These values are much closer to the errors for *HWind* (Table 4), which again can be seen as a baseline to which to compare the GAHM simulations. Taken together, these analyses show that the *HWind* hindcast is the best representation of the winds and water levels during Arthur in coastal NC. However, *GAHM(HWind)* also matches well to the

storm's behavior and effects on the coastal ocean, and thus GAHM can be used to explore forecast errors.

4.1.2. Forecasts

During Arthur, the ASGS system was running simulations of SWAN+ADCIRC to predict the storm-driven waves and flooding along coastal NC (http://nc-cera.renci.org). Using the forecast advisories issued by the NHC, those simulations were forced by vortex wind and pressure fields from the Asymmetric Holland Model (AHM, (Mattocks and Forbes, 2008; Mattocks et al., 2006)), the predecessor to GAHM. Herein, we evaluate the performance of GAHM by using the same forecast advisories as input, and thus these simulations can be considered as forecasts. While guidance was developed for all forecast advisories during the storm, we focus on three forecasts:

- Advisory 4, issued 2014/07/01/2100 UTC, about 54 h before landfall
- Advisory 8, issued 2014/07/02/2100 UTC, about 30 h before landfall
- Advisory 12, issued 2014/07/03/2100 UTC, about 6 h before landfall

As noted previously, the storm track was fairly consistent during the early forecasts, with a projected movement offshore of coastal NC, but then the storm track changed during the forecasts issued in the last 24 h before landfall, toward a projected landfall near Beaufort, NC.

These storm track errors cause variability in the wind and surge predictions (Fig. 8). In the earlier advisories 4 and 8, the hurricane-strength winds (with speeds larger than 32 m/s) are located offshore, while coastal NC is subjected to lesser winds of tropical-storm- or tropical-depression-strength (Fig. 8, left column). Wilmington and Cape Fear are forecast to experience maximum wind speeds of about 20 m/s, and the sounds and Outer Banks are forecast to experience maximum wind speeds of 25 – 30 m/s. By advisory 12, the track shows the storm's correct movement over Pamlico Sound, and thus the entire region is subjected to wind speeds corresponding to a Category 1 storm on the Saffir-Simpson scale. The predicted maximum wind speeds are almost 40 m/s along a swath from Beaufort through Oregon Inlet, and thus effectively doubled from the earlier forecasts.

The track predictions from the later forecast (e.g., NHC advisory 12, issued 6 h before initial landfall) are a better representation of the storm's movement near four stations: 41037 (27 miles SE of Wrightsville Beach, NC), BFTN7 (Beaufort, NC), CLKN7 (Cape Lookout, NC) and ORIN7 (Oregon Inlet Marina, NC). The sharp drop in wind speed at 2014/07/04/2345 UTC at these stations and the presence of a double peak (Fig. 9) can be attributed to the influence of the storm eye near these locations; this effect is well-represented by the model wind speeds. However, the model over-predicts the wind speeds. At station 41037, the peak wind speeds for the later forecast (NHC advisory 12) were about 35 m/s, which is larger than the model predictions of 22 m/s from the earlier NHC advisories 4 through 8, but closer to the observed value of 29 m/s. At station BFTN7, the peak wind speeds from the later forecast are 7 m/s larger than the observations, while the peak wind speeds from the earlier forecasts are smaller and occur later than the observations. At station ORIN7, for the earlier forecasts, the errors in the track predictions cause the absence of a double peak and lower predicted peak wind speeds. However, the RMS difference for forecast advisory 4 at these four stations is about 5 m/s and is smaller than that of forecast advisory 12. Thus, while the later forecast advisory 12 is a better representation of the storm's track near these stations, their *RMS* differences are larger due to over-predictions of the wind speeds as Arthur moved through the system.

The effect is reversed at stations located farther offshore. At station 41025 (Diamond Shoals, NC) located southwest of Hatteras Island, NC, the wind speeds decrease sharply at the peak to less than 15 m/s and less than 5 m/s for forecast advisories 4 and 8, respectively, before rising again (Fig. 9). This behavior is indicative of the eye of the storm being simulated at this location, due to the erroneous storm trajectories predicted to pass over this station. For these earlier forecasts, the wind speeds are higher than the observations by about 5 m/s. At station 41025, the *RMS* differences are about 5.2 m/s for advisories 4 and 8, but they increase to about 5.6 m/s for the later advisory 12, during which the peak wind speeds are over-predicted by 9 m/s. These comparisons indicate that errors in track predictions can lead to over- or under-prediction of wind speeds at locations far or near to the actual storm track.

The ocean responded differently to these wind predictions. In the earlier advisories 4 and 8, the winds are easterly and then northerly as the storm moved offshore, and thus water was pushed in a southwestward direction (Fig. 8, right column). Water levels were decreased in the eastern Pamlico and Albemarle Sounds, and increased in southwestern Pamlico Sound and the Neuse River estuary. The maximum water levels are about 1 m along the ocean-side of the Outer Banks between Capes Lookout and Hatteras, and about 1.5 m in southwest Pamlico Sound. By advisory 12, the predicted storm effects are increased throughout the region. Water levels higher than 2 m are pushed into the Neuse River and against the sound-side of Hatteras Island, and the maximum water levels have increased along the ocean-side of the Outer Banks. This later forecast is qualitatively similar to the wind and surge predictions in the hindcasts (Figs. 4 and 6).

Comparisons at 8 stations show the evolution of the water-level predictions (Fig. 10). At station 8656483 (Beaufort, NC), which is located near the path of the storm, the peak water levels predicted in the earlier advisories 4 and 8 were lower than the observed values by about 0.40 m. At station 8652587 (Oregon Inlet Marina), the forecasts showed a drawdown of as much as 0.5 m during advisories 4 and 8. However, there was a rise in water level of about 1.25 m at this location. This rise is evident in predictions based on later advisories (as in advisory 12), but the model under-predicts the observed peak surge by about 0.5 m, likely because this rise was not sufficient to counter the modeled drawdown of 0.25 m that occurred a few hours prior to the rise in surge. This drawdown was not observed and can be attributed to overestimation of the winds.

To quantify the change in model performance over time, the B_{MN} and *RMS* are computed in two ways. First, these quantities are computed relative to the observations at the 10 wind and 8 water-level stations.

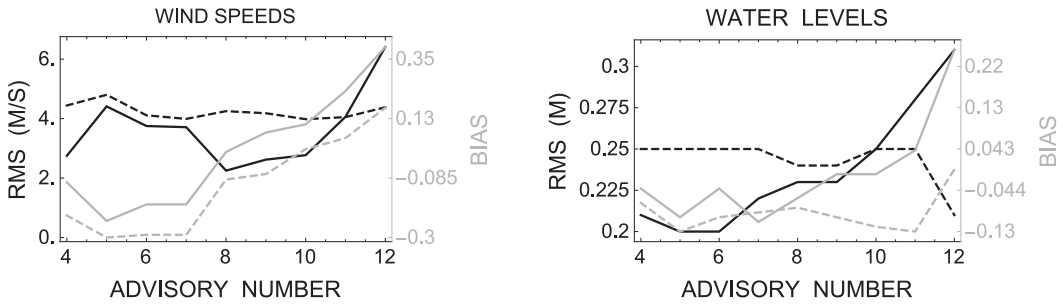

Fig. 11. Error statistics for the forecast simulations using NHC advisories 4 through 12. Columns correspond to (left) winds and (right) water levels. Error statistics are shown for (black) *RMS* and (gray) B_{MN}, with comparisons to (dashed) observations and (solid) *HWind* hindcast simulation.

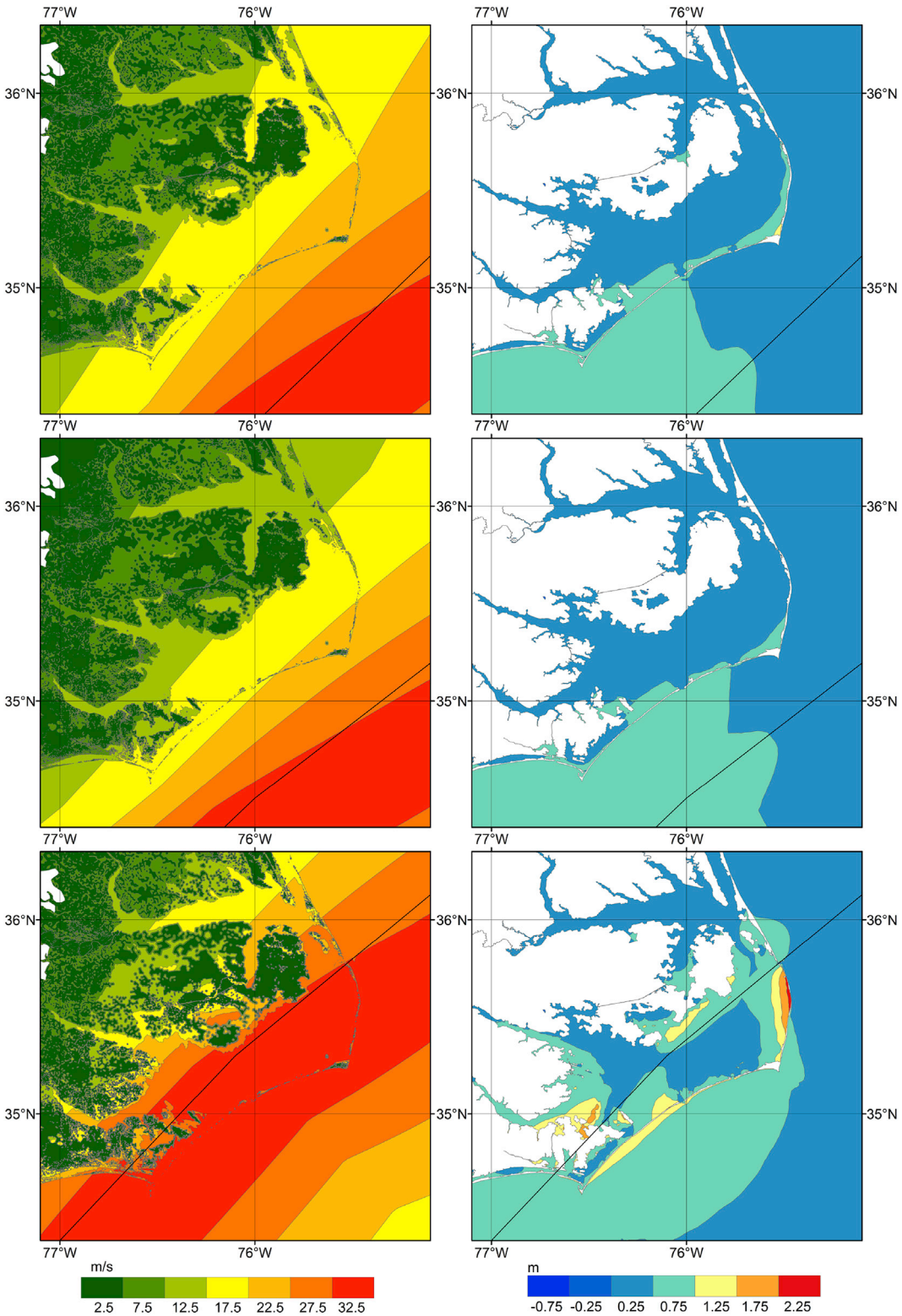

Fig. 12. Forecasts of winds (m/s) and water levels (m) during Arthur in coastal North Carolina, but with constant storm size and intensity parameters from HWind. Rows correspond to: (top) *GAHM(4,HWind)*, (middle) *GAHM(8,HWind)*, and (bottom) *GAHM(12,HWind)*. Columns correspond to: (left) maximum wind speeds, and (right) maximum water levels.

Error statistics were averaged in time at each station, and then averaged over the stations; these are the dashed lines in Fig. 11. Despite the improvement in storm track projections in the later advisories, the error statistics do not show any clear improvement. For the wind speeds, the *RMS* difference is relatively constant at 4 m/s, and for the water levels, the *RMS* difference is steady at 0.25 m until it decreases at the last advisory. Second, these quantities were computed relative to the peak values in the *HWind* hindcast simulation; these are the solid lines in Fig. 11. For the wind speeds, the peak values were compared at every point in the computational domain; for the peak water levels, the

comparison was limited to points with depths less than 10 m. For this comparison of peak values, there is a clear increase in the errors at the later advisories 10–12, during the day before the storm's initial landfall. The global RMS errors increase in NHC advisory 12 to 6.47 m/s for winds, and 0.31 m for water levels. The forecasts were not converging to the storm as represented by the *HWind* hindcast (*RMS* = 2.69 m/s for winds, *RMS* = 0.16 m for water levels).

4.2. Error due to storm track

To control for the relative effects of errors in storm track and storm strength, the forecast simulations were repeated, but with parameters from the *HWind* hindcast. To examine the affects of errors due to storm track, GAHM was employed with the storm track from each NHC forecast advisory, but with parameters for storm size and intensity from the HWind analysis product (as summarized in Table 3). For example, *GAHM(4,HWind)* denotes a simulation with the storm track from NHC forecast advisory 4, but parameters for storm size and intensity from the *HWind* hindcast. Thus, the same storm is applied on forecast tracks, which converge toward the true landfall location.

The power dissipation for *HWind* (about $1.87{\cdot}10^{12}$ watts) was similar to that for *GAHM(4)* (about $2.04{\cdot}10^{12}$ watts), and thus the projected storm size and wind speed were generally consistent at this time. The swath of hurricane-strength winds was located entirely offshore, and only the barrier islands and Pamlico Sound experienced tropical-storm-strength winds (Fig. 12, top left). For NHC advisory 8 issued 24 h later, there is a noticeable improvement in the maximum wind speeds, and thus the associated water-level response. For the *GAHM(8)* simulation (Fig. 8, middle row), the tropical-storm-strength winds larger than 18 m/s extended throughout coastal NC, and pushed water levels larger than 1.5 m in the southwest Pamlico Sound. For the *GAHM(8,HWind)* simulation (Fig. 12, middle row), the maximum wind speeds are much smaller in coastal NC, and the associated water-level response is negligible. The maximum wind speeds are also smaller for *GAHM(12,HWind)*, with hurricane-strength winds confined to the barrier islands and Pamlico Sound (Fig. 12, bottom row). The projected water levels have similar peak values of about 2 m, but these peaks are confined to smaller regions along the sound-side of Hatteras Island, and near the Neuse River estuary.

The error statistics show how the wind and water-level predictions are sensitive to track errors. For the wind speeds, the RMS and bias errors converge both with later advisories and landfall error (Fig. 13, left column). For the early advisories 4–7, the global RMS errors are larger than 5.6 m/s, but they decrease to 2.83 m/s for advisory 12, which is only slightly larger than the RMS error computed for *HWind* wind speeds (2.69 m/s, Table: 4). This convergence is linked to the landfall error, which decreases from 137 km for advisory 5 to less than 9 km for advisory 12. The global RMS errors for the wind speeds decrease gradually as the storm track shifted toward coastal NC.

The water levels did not converge gradually as the storm track is improved (Fig. 13, right column). Instead, the global RMS errors are relatively constant for advisories 4–11 at about 0.2 m, even as the landfall error decreases by more than 120 km. It is only during advisory 12, in which the projected track had the storm moving correctly over coastal NC, when the errors are improved. For *GAHM(12,HWind)*, the global RMS error improves to 0.13 m, and the global bias improves to 0.03. These statistics are slightly better than the computed RMS error and bias for the *HWind* water levels that are equal to 0.16 m and −0.17 respectively (Table 4). These results show the nonlinearity of the water-level response. The drop in both station and global RMS errors from *GAHM(11,HWind)* to *GAHM(12,HWind)* is attributed to differences in the tracks of advisories 11 and 12. The initial landfall error of about 15 km for advisory 11 is similar to the initial landfall error of less than 9 km for advisory 12, but their tracks diverge over coastal NC. The track of advisory 11 predicted the storm center to move along the eastern edge of Pamlico Sound with a potential landfall at Hatteras Island, thereby causing a significant drawdown in parts of the northern Pamlico Sound (not shown). Forecast corresponding to advisory 12, however, shifted the track west and provided a more accurate representation of the storm center's real path. Thus, in contrast to *GAHM(11,HWind)*, the entire eastern portion of the Pamlico Sound fall to the right of the storm center for *GAHM(12,HWind)* and experience positive surges, which are a better match to measured water levels and *HWind* hindcast results. As the storm size and intensity are held constant, and as the storm track is improved gradually, the water level predictions do not change until the wind speeds and directions are correct in coastal NC.

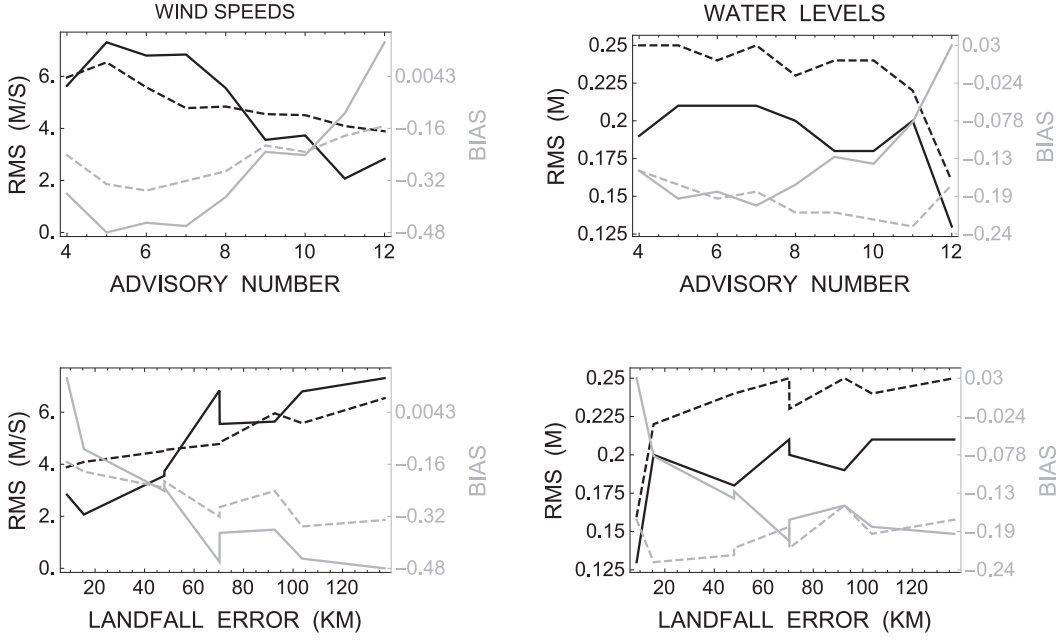

Fig. 13. Error statistics for the forecast simulations using NHC advisories 4 through 12 for storm track, but HWind parameters for storm size and intensity. Columns correspond to (left) winds and (right) water levels. Rows show the same information, but for (top) advisory number and (bottom) landfall error (km). Error statistics are shown for (black) *RMS* and (gray) B_{MN}, with comparisons to (dashed) observations and (solid) *HWind* hindcast simulation.

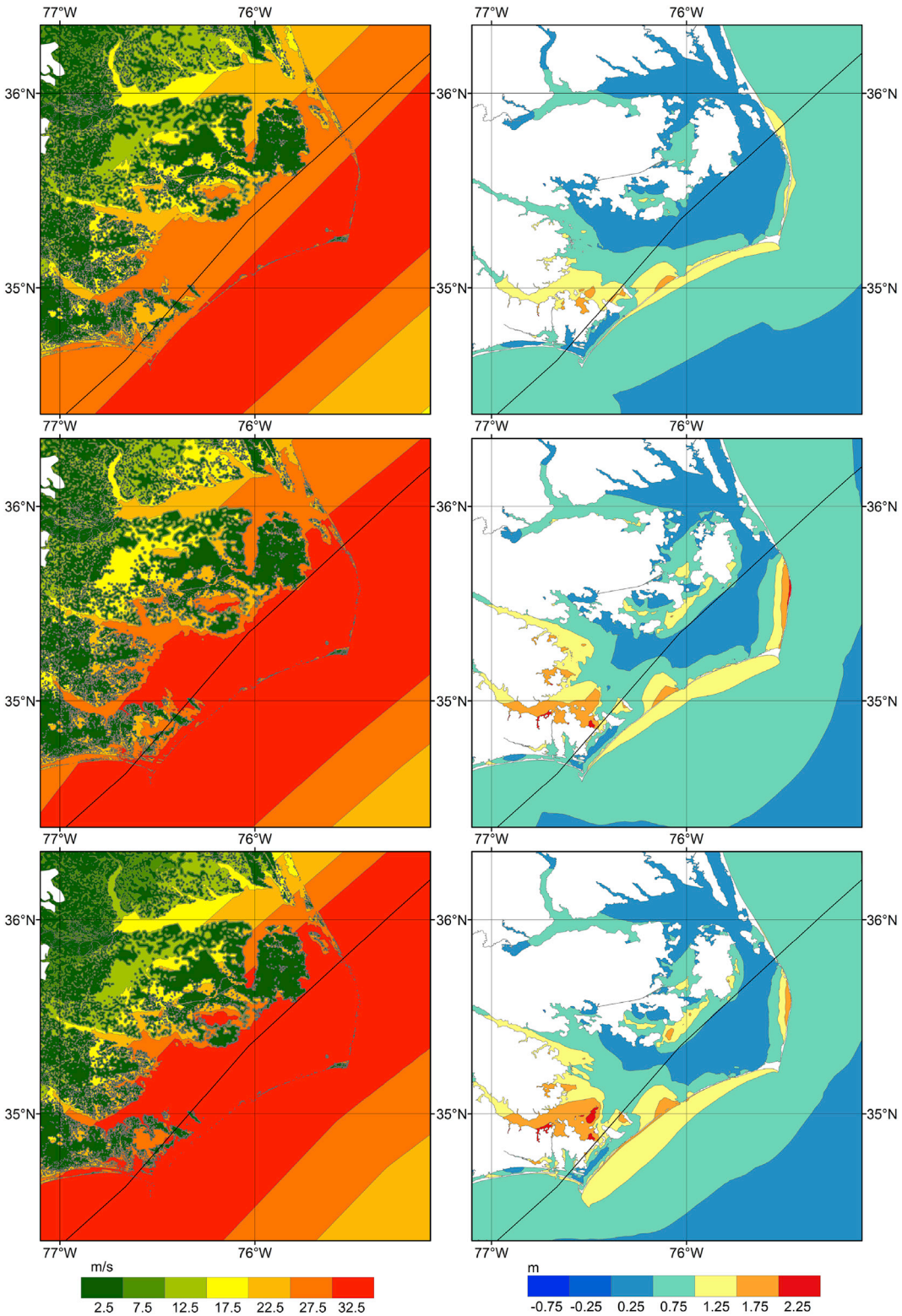

Fig. 14. Forecasts of winds (m/s) and water levels (m) during Arthur in coastal North Carolina, but with constant track information from HWind. Rows correspond to: (top) *GAHM(HWind,4)*, (middle) *GAHM(HWind,8)*, and (bottom) *GAHM(HWind,12)*. Columns correspond to: (left) maximum wind speeds, and (right) maximum water levels.

4.3. Error due to storm size and intensity

As the forecast track was converging to the correct landfall location, the forecast storm was increasing in power dissipation (Fig. 3). By advisory 12, the forecast power dissipation of $3.10{\cdot}10^{12}$ watts was more than 50 percent larger than the post storm determined power dissipation of $1.87{\cdot}10^{12}$ watts in the *HWind* simulation. To examine the effects of this overestimation of storm power on the surge and coastal flooding, we repeated the forecast simulation while holding the storm track constant as determined from the HWind fields (see Table 3). For example,

GAHM(HWind,4) denotes a simulation with parameters for storm size and intensity from NHC forecast advisory 4, but the storm track from the *HWind* hindcast. Thus, the same track is used for the forecast storms, which increases in power dissipation.

These simulations show the growth of the storm in size and intensity in subsequent forecasts (Fig. 14, left column). In *GAHM(HWind,4)*, much of the NC coastal regions see maximum wind speeds greater than 18 m/s (corresponding to a tropical storm), but the largest maximum wind speeds greater than 33 m/s (Category 1 hurricane) are confined over the Outer Banks and Cape Hatteras. In the later forecast advisories, this region of hurricane-strength maximum winds is expanded to include all of Pamlico Sound and, in *GAHM(HWind,12)*, regions to the west of the *HWind* hindcast track. There is a correlation between the forecast increase in power dissipation and the global root-mean-square and bias errors in the simulated wind fields (Fig. 15, left column). As the power dissipation is increased, the global *RMS* errors increase from about 3.6 m/s for advisories 4 and 5, to more than 5 m/s for advisories 11 and 12. This correlation is not perfect, e.g., the largest global *RMS* error is observed for advisory 11, when the power dissipation was $2.6{\cdot}10^{12}$ watts and thus less than its maximum value. And there is no correlation for the error statistics computed relative to the observations, e.g., their *RMS* errors are consistently $4-5$ m/s, which is larger than the RMS errors for *HWind* wind speeds (2.69 m/s, Table 4), regardless of the power dissipation of the forecast storm. However, the global error statistics do increase as the forecast storms increase in strength.

A similar behavior can be observed for the maximum water levels (Fig. 14). In *GAHM(HWind,4)*, the largest water levels of 1.5 m or greater are confined to southwest Pamlico Sound and the Neuse River estuary. In the later forecast advisories, these water levels increase in magnitude, similar peaks in water levels are evident on the sound-side of Hatteras Island north of its cape, and on the ocean-side of the Outer Banks between Capes Lookout and Hatteras. As the forecast storms increase in power, they push water more effectively. This correlation is seen in the error statistics for the water levels (Fig. 15, right column). The global *RMS* errors increase from about 0.24 m in advisories 4 and 5, to about 0.28 m in advisories 11 and 12, and the global bias increases from about 0.03 to about 0.15. The RMS errors computed relative to observations are larger than that of *HWind* water levels (0.16 m, Table 4) and stay above 0.25 m for most of the advisories and rise up to 0.3 m for advisory 12. These increases correlate with the increasing power dissipation, although not as strongly as for the wind speeds, thus indicating the nonlinearity of the coastal ocean response.

5. Conclusions

The SWAN+ADCIRC modeling system was applied to high-resolution simulations of storm surge and coastal flooding during Hurricane Arthur (2014). The surge model was forced with wind velocities from the HWind analysis product, and surface pressures and wind velocities from the GAHM parametric vortex model. The effects of the atmospheric forcing were evaluated for hindcasts using the best-available information after the storm, as well as for forecasts containing information released as the storm approached NC. Then, by repeating the forecast simulations and replacing their uncertainties with known information from after the storm, we quantified the errors in computed wind speeds and water levels due to errors in storm power and track. Our findings can be summarized as follows:

1. *The HWind simulation was the best representation of Arthur's wind hazards and associated ocean response, but GAHM(HWind) was a close approximation.* The *HWind* wind fields and water levels were the best match to observations at stations offshore and in coastal NC. When GAHM was used with the NHC best-track information as *GAHM(BT)*, it did not match as well at the observations, but its performance improved considerably when the best-track information was replaced with parameters from *HWind* as *GAHM(HWind)*. Thus, given correct information about the storm's size, intensity, and track, GAHM can reproduce the key characteristics of the storm.

2. *Forecasts of wind speeds and water levels became less accurate (i.e deviated more from post-storm determined HWind results)* as the storm approached landfall. For wind speeds, the global root-mean-square error more than doubled, while for the water levels, the global root-mean-square error increased by 50 percent. This deterioration in forecast accuracy was due to the combined errors in storm track and power dissipation (a measure of combined size and intensity). The storm track improved in later advisories, but the forecasted intensity (as represented by the PD) was significantly larger than the post-storm determined

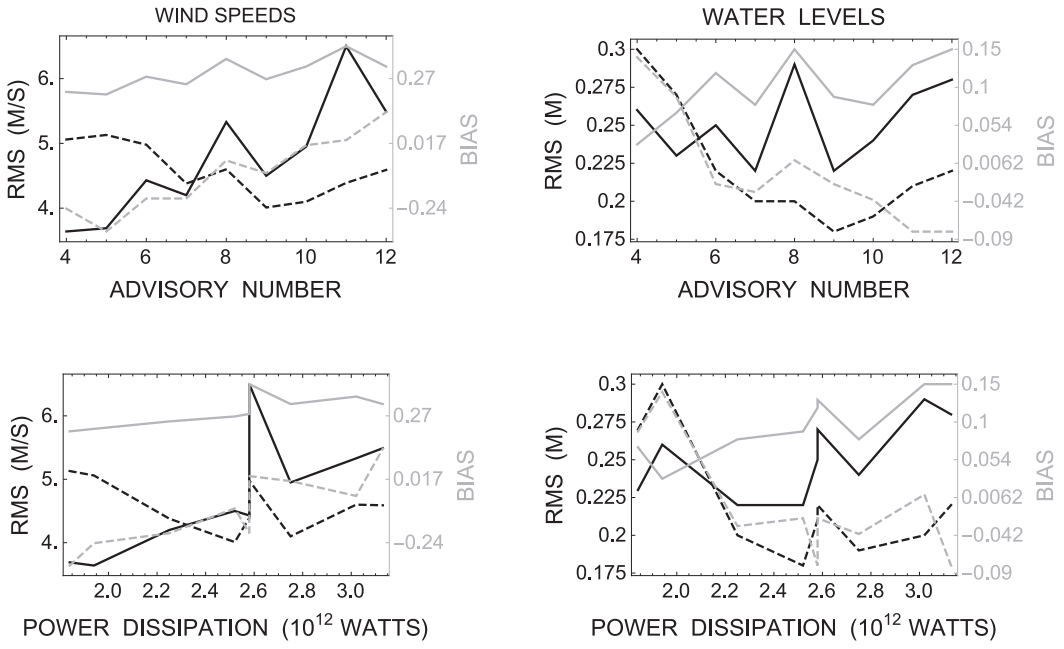

Fig. 15. Error statistics for the forecast simulations using NHC advisories 4 through 12 for storm size and intensity, but HWind parameters for storm track. Columns correspond to (left) winds and (right) water levels. Rows show the same information, but for (top) advisory number and (bottom) power dissipation (10^{12} watts). Error statistics are shown for (black) *RMS* and (gray) B_{MN}, with comparisons to (dashed) observations and (solid) *HWind* hindcast simulation.

intensity. This resulted in forecasts that overpredicted the peak winds and surge.

3. *As the forecast storm track and intensity errors increase, the errors in forecast wind speeds also increase, but the errors in forecast water levels remain relatively consistent.* By using parameters from the HWind analysis product, we repeated the forecast simulations to control for these errors. The wind-speed errors decreased significantly as the storm track converged to the correct landfall location, and they increased significantly as the storm was projected to grow in size and intensity. The water-level errors responded nonlinearly, with only a late improvement when the track became 'correct,' and only a slight worsening as the storm became too powerful. The ocean response will also depend on the tide level, coastline geometry, and other characteristics of the coast.

Although this study is specific to Arthur, it demonstrates the potential for forecast errors in peak wind speeds and surge levels due to separate errors in storm track and power. It is typical for Atlantic storms to follow a shore-parallel track and move near or over coastal NC, such as Irene (2011) and Hermine and Matthew (2016), and thus we are encouraged to continue improving our modeling system to advance storm preparation efforts in North Carolina. Future work will focus on improving the computational speed to make forecast guidance available sooner and to benefit ensemble forecasting, and on improving the communication of forecasts and their potential errors to local stakeholders.

Acknowledgements

This work was made possible by grants from NOAA through the North Carolina Sea Grant, and from the Gulf of Mexico Research Initiative (GoMRI) through the Consortium for Advanced Research on Transport of Hydrocarbon in the Environment (CARTHE). Data are publicly available through the Gulf of Mexico Research Initiative Information & Data Cooperative (GRIIDC) at https://data.gulfresearchinitiative.org and with the following Digital Object Identifiers (DOIs): 10.7266/N7RR1WM1 (Cyriac and Dietrich, 2018a), 10.7266/N71J988J (Cyriac and Dietrich, 2018b), 10.7266/N72B8WJF (Cyriac and Dietrich, 2018c), 10.7266/N7XK8D30 (Cyriac and Dietrich, 2018d). This material is also based upon work supported by the U.S. Department of Homeland Security under Grant Award Number 2015-ST-061-ND0001-01. The views and conclusions contained in this document are those of the authors and should not be interpreted as necessarily representing the official policies, either expressed or implied, of the U.S. Department of Homeland Security. Geospatial visualizations were produced using Kalpana (https://ccht.ccee.ncsu.edu/kalpana/).

References

Atkinson, J.H., Smith, J.M., Bender, C., 2013. Sea-level rise effects on storm surge and nearshore waves on the Texas coast: influence of landscape and storm characteristics. J. Waterw. Port Coast. Ocean Eng. 139, 98–117.

Barnes, J., 2013. North Carolina's Hurricane History, fourth ed. University of North Carolina Press.

Berg, R., 2015. Tropical Cyclone Report, Hurricane Arthur, 1–5 July 2015, Tech. Rep. National Hurricane Center.

Bhaskaran, P.K., Nayak, S., Bonthu, S.R., Murthy, P.L.N., Sen, D., 2013. Performance and validation of a coupled parallel ADCIRC-SWAN model for THANE cyclone in the Bay of Bengal. Environ. Fluid Mech. 13, 601–623.

Blanton, B., Luettich, R.A., 2008. North Carolina Coastal Flood Analysis System: Model Grid Generation, Tech. Rep. TR-08–05. Renaissance Computing Institute.

Blanton, B., Madry, S., Gallupi, K., Gamiel, K., Lander, H., Reed, M., Stillwell, L., Blanchard-Montogomery, M., Luettich, R., Mattocks, C., Fulcher, C., Vickery, P., Hanson, J., Devaliere, E., McCormick, J., 2008. Report for State of North Carolina Floodplain Mapping Project Costal Flood Analysis System, Tech. Rep. TR-08–08. Renaissance Computing Institute.

Blanton, B.O., McGee, J., Fleming, J.G., Kaiser, C., Kaiser, H., Lander, H., Luettich, R.A., Dresback, K.M., Kolar, R.L., 2012. Urgent computing of storm surge for North Carolina's coast. In: Proceedings of the International Conference on Computational Science, vol. 9, pp. 1677–1686.

Blanton, B.O., Luettich, R.A., Hanson, J.L., Vickery, P., Slover, K., Langan, T., 2012. North Carolina Floodplain Mapping Program, Coastal Flood Insurance Study: Production Simulations and Statistical Analyses, Tech. Rep. TR-12–06. Renaissance Computing Institute.

Bunya, S., Dietrich, J.C., Westerink, J.J., Ebersole, B.A., Smith, J.M., Atkinson, J.H., Jensen, R.E., Resio, D.T., Luettich, R.A., Dawson, C.N., Cardone, V.J., Cox, A.T., Powell, M.D., Westerink, H.J., Roberts, H.J., 2010. A high-resolution coupled riverine flow, tide, wind, wind wave and storm surge model for southern Louisiana and Mississippi: Part I – model development and validation. Mon. Weather Rev. 138, 345–377.

Cheung, K.F., Phadke, A.C., Wei, Y., Rojas, R., Douyere, Y.J.M., Martino, C.D., Houston, S.H., Liu, P.L.F., Lynett, P.J., Dodd, N., Liao, S., Nakazaki, E., 2003. Modeling of storm-induced coastal flooding for emergency management. Ocean Eng. 30, 1353–1386.

Cyriac, R., Dietrich, J.C., 2018a. CARTHE-II: Coupled wave-circulation results from the SWAN+ADCIRC hindcast models for the North Carolina coast during Hurricane Arthur (2014), Distributed by: Gulf of Mexico Research Initiative Information and Data Cooperative (GRIIDC). Harte Research Institute, Texas A&M University - Corpus Christi. Available from: https://data.gulfresearchinitiative.org/data/R4.x265.246:0001.

Cyriac, R., Dietrich, J.C., 2018b. CARTHE-II: Coupled wave-circulation results from the SWAN+ADCIRC models for the North Carolina coast during Hurricane Arthur (2014) forced by NHC advisories, best track and modified HWind data, Distributed by: Gulf of Mexico Research Initiative Information and Data Cooperative (GRIIDC). Harte Research Institute, Texas A&M University - Corpus Christi. Available from: https://data.gulfresearchinitiative.org/data/R4.x265.000:0055.

Cyriac, R., Dietrich, J.C., 2018c. CARTHE-II: Coupled wave-circulation results from the SWAN+ADCIRC models to analyze errors in forecast storm strength during Hurricane Arthur (2014), Distributed by: Gulf of Mexico Research Initiative Information and Data Cooperative (GRIIDC). Harte Research Institute, Texas A&M University - Corpus Christi. Available from: https://data.gulfresearchinitiative.org/data/R4. x265.000:0056.

Cyriac, R., Dietrich, J.C., 2018d. CARTHE-II: Coupled wave-circulation results from the SWAN+ADCIRC models to analyze errors in forecast storm track during Hurricane Arthur (2014), Distributed by: Gulf of Mexico Research Initiative Information and Data Cooperative (GRIIDC). Harte Research Institute, Texas A&M University - Corpus Christi. Available from: https://data.gulfresearchinitiative.org/data/R4.x265.000:0057.

Dawson, C.N., Westerink, J.J., Feyen, J.C., Pothina, D., 2006. Continuous, discontinuous and coupled discontinuous-continuous Galerkin finite element methods for the shallow water equations. Int. J. Numer. Meth. Fluid. 52, 63–88.

Dietrich, J.C., Westerink, J.J., Kennedy, A.B., Smith, J.M., Jensen, R.E., Zijlema, M., Holthuijsen, L.H., Dawson, C.N., Luettich, R.A., Powell, M.D., Cardone, V.J., Cox, A.T., Stone, G.W., Pourtaheri, H., Hope, M.E., Tanaka, S., Westerink, L.G., Westerink, H.J., Cobell, Z., Gustav, Hurricane, 2008. waves and storm surge: Hindcast, validation and synoptic analysis in southern Louisiana. Mon. Weather Rev. 139 (2011), 2488–2522.

Dietrich, J.C., Bunya, S., Westerink, J.J., Ebersole, B.A., Smith, J.M., Atkinson, J.H., Jensen, R.E., Resio, D.T., Luettich, R.A., Dawson, C.N., Cardone, V.J., Cox, A.T., Powell, M.D., Westerink, H.J., Roberts, H.J., 2010. A high-resolution coupled riverine flow, tide, wind, wind wave and storm surge model for southern Louisiana and Mississippi: Part II – synoptic description and analysis of Hurricanes Katrina and Rita. Mon. Weather Rev. 138, 378–404.

Dietrich, J.C., Zijlema, M., Westerink, J.J., Holthuijsen, L.H., Dawson, C.N., Luettich, R.A., Jensen, R.E., Smith, J.M., Stelling, G.S., Stone, G.W., 2011. Modeling hurricane waves and storm surge using integrally-coupled, scalable computations. Coast Eng. 58, 45–65.

Dietrich, J.C., Muhammad, A., Curcic, M., Fathi, A., Dawson, C.N., Chen, S.S., Luettich, R.A., 2012. Sensitivity of storm surge predictions to atmospheric forcing during Hurricane Isaac. J. Waterw. Port Coast. Ocean Eng. 144 (1).

Dietrich, J.C., Tanaka, S., Westerink, J.J., Dawson, C.N., Luettich, R.A., Zijlema, M., Holthuijsen, L.H., Smith, J.M., Westerink, L.G., Westerink, H.J., 2012. Performance of the unstructured-mesh, SWAN+ADCIRC model in computing hurricane waves and surge. J. Sci. Comput. 52, 468–497.

Dietrich, J.C., Dawson, C.N., Proft, J., Howard, M.T., Wells, G., Fleming, J.G., Luettich, R.A., Westerink, J.J., Cobell, Z., Vitse, M., 2013. Real-time forecasting and visualization of hurricane waves and storm surge using SWAN+ADCIRC and FigureGen. In: Dawson, C.N., Gerritsen, M. (Eds.), Computational Challenges in the Geosciences, pp. 49–70.

Dietrich, J.C., Zijlema, M., Allier, P.E., Holthuijsen, L.H., Booij, N., Meixner, J.D., Proft, J.K., Dawson, C.N., Bender, C.J., Naimaster, A., Smith, J.M., Westerink, J.J., 2013. Limiters for spectral propagation velocities in SWAN. Ocean Model. 70, 85–102.

DiNapoli, S.M., Bourassa, M.A., Powell, M.D., 2012. Uncertainty and intercalibration analysis of H*Wind. J. Atmos. Ocean. Technol. 29, 822–833.

Dresback, K.M., Fleming, J.G., Blanton, B.O., Kaiser, C., Gourley, J.J., Tromble, E.M., Luettich, R.A., Kolar, R.L., Hong, Y., Van Cooten, S., Vergara, H.J., Flamig, Z., Lander, H.M., Kelleher, K.E., Nemunaitis-Monroe, K.L., 2011. Skill assessment of a real-time forecast system utilizing a coupled hydrologic and coastal hydrodynamic model during Hurricane Irene. Continent. Shelf Res. 71 (2013), 78–94.

Emanuel, K., 2005. Increasing destructiveness of tropical cyclones over the past 30 years. Nature 436, 686–688.

Fleming, J., Fulcher, C., Luettich, R.A., Estrade, B., Allen, G., Winer, H., 2007. A real time storm surge forecasting system using ADCIRC. Estuar. Coas. Model. 2008, 893–912.

Forbes, C., Luettich, R.A., Mattocks, C.A., Westerink, J.J., 2010. A retrospective evaluation of the storm surge produced by Hurricane Gustav (2008): forecast and hindcast results. Weather Forecast. 25, 1577–1602.

Garratt, J.R., 1977. Review of drag coefficients over oceans and continents. Mon. Weather Rev. 105, 915–929.

Holland, R.W., 1980. An analytic model of the wind and pressure profiles in hurricanes. Mon. Weather Rev. 108, 1212–1218.
Hope, M.E., Westerink, J.J., Kennedy, A.B., Kerr, P.C., Dietrich, J.C., Dawson, C.N., Bender, C.J., Smith, J.M., Jensen, R.E., Zijlema, M., Holthuijsen, L.H., Luettich Jr., R.A., Powell, M.D., Cardone, V.J., Cox, A.T., Pourtaheri, H., Roberts, H.J., Atkinson, J.H., Tanaka, S., Westerink, H.J., Westerink, L.G., Hindcast and Validation of Hurricane Ike, 2008. Waves, forerunner, and storm surge. J. Geophys. Res. Oceans 118 (2013), 4424–4460.
Kerr, P.C., Donahue, A.S., Westerink, J.J., Luettich, R.A., Zheng, L.Y., Weisburg, R.H., Huang, Y., Wang, H.V., Teng, Y., Forrest, D.R., Roland, A., Haase, A.T., Kramer, A.W., Taylor, A.A., Rhome, J.R., Feyen, J.C., Signell, R.P., Hanson, J.L., Hope, M.E., Estes, R.M., Dominguez, R.A., Dunbar, R.P., Semeraro, L.N., Westerink, H.J., Kennedy, A.B., Smith, J.M., Powell, M.D., Cardone, V.J., Cox, A.T., 2013. U.S. IOOS coastal and ocean modeling testbed: inter-model evaluation of tides, waves, and hurricane surge in the Gulf of Mexico. J. Geophys. Res. Oceans 118, 5129–5172.
Lin, N., Emmanuel, K., 2016. Grey swan tropical cyclones. Nat. Clim. Change 6, 106–111.
Lin, N., Emmanuel, K., Oppenheimer, M., Vanmarcke, E., 2012. Physically based assessment of hurricane surge threat under climate change. Nat. Clim. Change 2, 462–467.
Luettich, R.A., Westerink, J.J., 2004. Formulation and Numerical Implementation of the 2D/3D ADCIRC Finite Element Model Version 44. XX. http://adcirc.org/adcirc_theory_2004_12_08.pdf.
Mattocks, C., Forbes, C., 2008. A real-time, event-triggered storm surge forecasting system for the state of North Carolina. Ocean Model. 25, 95–119.
Mattocks, C., Forbes, C., Ran, L., 2006. Design and Implementation of a Real-time Storm Surge and Flood Forecasting Capability for the State of North Carolina, Tech. Rep. University of North Carolina.
Murty, P.L.N., Sandhya, K.G., Bhaskaran, P.K., Jose, F., Gayathri, R., Balakrishnan Nair, T.M., Srinivasa Kumar, T., Shenoi, S.S.C., 2014. A coupled hydrodynamic modeling system for PHAILIN cyclone in the Bay of Bengal. Coast Eng. 93, 71–81.
National Hurricane Center, 2017. Official Average Track Errors [Retrieved 21 August 2017]. http://www.nhc.noaa.gov/verification/figs/ALtkerr_decade_noTD.jpg.
Peng, M., Xie, L., Pietrafesa, L.J., 2004. A numerical study of storm surge and inundation in the Croatan-Albemarle-Pamlico estuary system. Estuar. Coast. Shelf Sci. 59, 121–137.
Peng, M., Xie, L., Pietrafesa, L.J., 2006. Tropical cyclone induced asymmetry of sea level surge and fall and its presentation in a storm surge model with parametric wind fields. Ocean Model. 14, 81–101.
Powell, M.D., Houston, S.H., Reinhold, T.A., 1996. Hurricane Andrew's landfall in South Florida, Part I: standardizing measurements for documentation of surface wind fields. Weather Forecast. 11, 304–328.
Powell, M.D., Houston, S.H., Amat, L.R., Morisseau-Leroy, N., 1998. The HRD real-time hurricane wind analysis system. J. Wind Eng. Ind. Aerod. 77–78, 53–64.
Resio, D.T., Powell, N.J., Cialone, M.A., Das, H.S., Westerink, J.J., 2017. Quantifying impacts of forecast uncertainties on predicted storm surges. Nat. Hazards 88, 1423–1449.
State Climate Office of North Carolina, 2017 [Retrieved 21 June 2017]. http://climate.ncsu.edu/climate/hurricanes/statistics.php.
Vickery, P., Skerlj, P., 2005. Hurricane gust factors revisited. J. Struct. Eng. 131, 825–832.
Westerink, J.J., Luettich Jr., R.A., Feyen, J.C., Atkinson, J.H., Dawson, C.N., Roberts, H.J., Powell, M.D., Dunion, J.P., Kubatko, E.J., Pourtaheri, H., 2008. A basin to channel scale unstructured grid hurricane storm surge model applied to southern Louisiana. Mon. Weather Rev. 136, 833–864.
Xie, L., Bao, S., Pietrafesa, L.J., Foley, K., Fuentes, M., 2006. A real-time hurricane surface wind forecasting model: formulation and verification. Mon. Weather Rev. 134, 1355–1370.
Zhong, L., Li, M., Zhang, D.-L., 2010. How do uncertainties in hurricane model forecasts affect storm surge predictions in a semi-enclosed bay? Estuar. Coast Shelf Sci. 90, 61–72.